Synthesis and X-ray Crystallographic Studies of Diacetylenic Molecules Bearing Triorganosilyl, Triorganostannyl, and Diorganophosphanyl Substituents. Investigation of Their Solid-State and Molten-State Polymerization

Francis Carré, Nathalie Devylder, Sylvain G. Dutremez,* Christian Guérin, Bernard J. L. Henner, Agnès Jolivet, and Véronique Tomberli

Laboratoire "Chimie Moléculaire et Organisation du Solide", UMR 5637, Université Montpellier II, Case Courrier 007, Place E. Bataillon, 34095 Montpellier Cedex 5, France

Françoise Dahan

Laboratoire de Chimie de Coordination du CNRS, UPR 8241, Liée par Conventions à l'Université Paul Sabatier et à l'Institut National Polytechnique de Toulouse, 205 Route de Narbonne, 31077 Toulouse Cedex 4, France

Received November 6, 2002

The following series of silicon-containing diacetylenes has been prepared: $R_3SiC{\equiv}CC{\equiv}CSiR_3$ ($R_3 = Me_3$ (**2a**); $R_3 = Me_2Ph$ (**2b**); $R_3 = MePh_2$ (**2c**); $R_3 = Ph_3$ (**2d**)), *rac*-MePhNpSiC≡CC≡CSiMePhNp (**2e**: Np = 1-naphthyl), (*R*,*R*)-(+)-MePhNpSiC≡CC≡CSiMePhNp (**2e***), *rac*-$Ph_3SiC{\equiv}CC{\equiv}CSiMePhNp$ (**3**), (*R*)-(+)-$Ph_3SiC{\equiv}CC{\equiv}CSiMePhNp$ (**3***), $R_3SiCH_2C{\equiv}CC{\equiv}CCH_2SiR_3$ ($R_3 = Me_3$ (**4a**); $R_3 = Ph_3$ (**4b**)), $R_2HSiC{\equiv}CC{\equiv}CSiHR_2$ ($R_2 = Me_2$ (**5a**); $R_2 = Ph_2$ (**5b**)), $R_3SiC{\equiv}CC{\equiv}CH$ ($R_3 = Me_3$ (**6a**); $R_3 = Ph_3$ (**6b**)), and *rac*-MePhNpSiC≡CC≡CH (**6c**). Single-crystal X-ray diffraction analyses were performed on **2a**, **2d**, **2e***, **4a**, and **4b** to determine the $R_{1,4}$ distance and the angle γ between neighboring diacetylenic rods in the solid. Diacetylenes **2a**, **2e***, and **4a** were tested for γ-ray and heat-induced solid-state polymerization reactivity, and in accordance with the X-ray results, polymerization was not observed. Terminal diyne **6c** showed no polymerization activity upon irradiation with a 100 krad dose of γ-rays but slowly polymerized in the solid state when heated to 70 °C for 13 days. Following a preliminary investigation of **2a**, **2d**, **2e**, **2e***, **3***, **4a**, **4b**, **5a**, **5b**, **6a**, **6b**, and **6c** by differential scanning calorimetry (DSC), these diynes were polymerized in the molten state or just below melting. MALDI-TOF mass spectrometry shows that the polymers consist of mixtures of oligomers with 2 to 10 repeat units. The constituting motif of these oligomers (enyne, butatriene, polyaromatic) was elucidated by use of infrared and solution and solid-state multinuclear NMR spectroscopies. Polymerization experiments were also carried out on $Me_3SnC{\equiv}CC{\equiv}CSnMe_3$ (**7a**), $Ph_3SnC{\equiv}CC{\equiv}CSnPh_3$ (**7b**), and $Ph_2PC{\equiv}CC{\equiv}CPPh_2$ (**8**), and the results of these experiments are compared with the polymerization results of their silicon-containing analogues. A 1,4-addition process takes place with **2a**, **2d**, **2e**, **2e***, **3***, **5a**, **5b**, **7a**, **7b**, and **8**, leading to butatriene and/or enyne structures. A 1,2-addition process is operative in the case of monosilylated derivatives **6a**, **6b**, and **6c**, giving acetylenic polyenes. Molten-state polymerization of **4a** and **4b** gives polyaromatic structures.

Introduction

Diacetylenic molecules in which the C_4 fragment is attached to one or two main group elements have been known for quite some time,[1] and several of them, e.g., $Me_3SiC{\equiv}CC{\equiv}CSiMe_3$ and $Ph_2PC{\equiv}CC{\equiv}CPPh_2$, have been used as ligands in transition metal chemistry.[2,3] Also, trimethylsilyl- and triisopropylsilyl-terminated diynes are commonly employed as synthons for the elaboration of carbon-rich networks,[4] and $Me_3SnC{\equiv}CC{\equiv}CSnMe_3$ has been used to prepare extended metal-polyyne polymers.[5] However, not much is known about the solid-state structures of these molecules, and interestingly, only a few of them have been characterized crystallographically.[6] Such information is quite valuable

* To whom correspondence should be addressed. Fax: (33) 4 67 14 38 52. E-mail: dutremez@univ-montp2.fr.

(1) (a) Hartmann, H.; Dietz, E.; Komorniczyk, K.; Reiss, W. *Naturwissenschaften* **1961**, *48*, 570. (b) Hartmann, H.; Komorniczyk, K. *Naturwissenschaften* **1964**, *51*, 214. (c) Hartmann, H.; Wagner, H.; Karbstein, B.; el A'ssar, M. K.; Reiss, W. *Naturwissenschaften* **1964**, *51*, 215. (d) Le Quan, M.; Cadiot, P. *Bull. Soc. Chim. Fr.* **1965**, 35. (e) Charrier, C.; Chodkiewicz, W.; Cadiot, P. *Bull. Soc. Chim. Fr.* **1966**, 1002. (f) Davidsohn, W. E.; Henry, M. C. *Chem. Rev.* **1967**, *67*, 73. (g) Bock, H.; Seidl, H. *J. Chem. Soc.* (*B*) **1968**, 1158. (h) Parnell, D. R.; Macaione, D. P. *J. Polym. Sci., Polym. Chem. Ed.* **1973**, *11*, 1107. (i) Nakovich, J., Jr.; Shook, S. D.; Miller, F. A.; Parnell, D. R.; Sacher, R. E. *Spectrochim. Acta, Part A* **1979**, *35*, 495.

10.1021/om020926a CCC: $25.00
Publication on Web 04/18/2003

in the area of supramolecular chemistry: we published recently the results of a study concerning the structural characterization of diacetylenic molecules possessing MR_3 moieties (M = Sn, Si; R = alkyl, aryl) and showed that some of these compounds were capable of including solvent molecules to produce host−guest complexes.[7] Also, the knowledge of the solid-state structures of diacetylenic molecules is desirable if topochemical polymerization is envisaged.[8] Such information has proven quite helpful to understand the thermal and/or photochemical solid-state polymerizability of certain diacetylenes.

In a related area, we have previously reported on the thermal behavior of poly[(silylene)diethynylenes)] (**1**) and shown that these polymers were viable precursors for the preparation of SiC-based ceramics.[9] The high ceramic yields that were observed were ascribed to 1,4-polymerization of the triple bonds between 200 and 300 °C, giving a cross-linked network that prevents volatile species containing silicon from being lost.

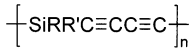

1

R = R' = Me, Ph, $SiMe_3$
R = Me; R' = Ph

We have engaged in the study of this cross-linking step using monomeric diacetylenic molecules with triorganosilyl substituents as models. These systems are simpler than poly[(silylene)diethynylenes], and the large panel of organic groups that can be attached to silicon gives access to a great deal of variations. Another asset of these well-defined molecular species is the greater ease to get a solid-state structure by single-crystal X-ray diffraction as compared to polymers.

Chart 1

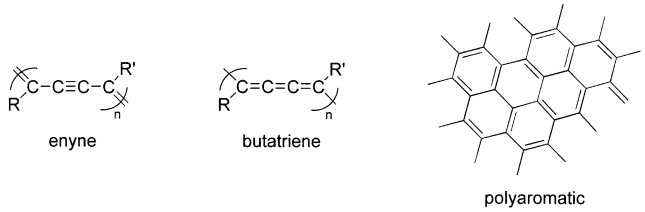

The first main focus of this paper is to establish a correlation between the organization of these 1,4-bis(triorganosilyl)buta-1,3-diynes in the crystal and their ability to polymerize in the solid state.[10]

Furthermore, as diacetylene polymerization can also be accomplished in the molten state,[11] this aspect is developed in the second part of this work. The objectives were to find the conditions for such polymerization to occur and determine the structures (enyne, butatriene, polyaromatic) of the resulting polymers (Chart 1). The knowledge of the structure of the final polymer is a valuable piece of information to have, as delocalization of the π-electrons is different in enyne, butatriene, or polyaromatic assemblies, and properties such as third-order optical nonlinearity depend strongly on efficient π-electron delocalization.[12]

(2) (a) Magnus, P.; Becker, D. P. *J. Chem. Soc., Chem. Commun.* **1985**, 640. (b) Klein, H.-F.; Schwind, M.; Flörke, U.; Haupt, H.-J. *Inorg. Chim. Acta* **1993**, *207*, 79. (c) Deeming, A. J.; Felix, M. S. B.; Nuel, D. *Inorg. Chim. Acta* **1993**, *213*, 3. (d) Rappert, T.; Nürnberg, O.; Werner, H. *Organometallics* **1993**, *12*, 1359. (e) Maekawa, M.; Munakata, M.; Kuroda-Sowa, T.; Hachiya, K. *Inorg. Chim. Acta* **1995**, *236*, 181. (f) Maekawa, M.; Munakata, M.; Kuroda-Sowa, T.; Hachiya, K. *Polyhedron* **1995**, *14*, 2879. (g) Lang, H.; Blau, S.; Rheinwald, G.; Zsolnai, L. *J. Organomet. Chem.* **1995**, *494*, 65. (h) Rosenthal, U.; Pulst, S.; Arndt, P.; Baumann, W.; Tillack, A.; Kempe, R. *Z. Naturforsch., B* **1995**, *50*, 368. (i) Rosenthal, U.; Pulst, S.; Arndt, P.; Baumann, W.; Tillack, A.; Kempe, R. *Z. Naturforsch., B* **1995**, *50*, 377. (j) Gauss, C.; Veghini, D.; Berke, H. *Chem. Ber./Recl.* **1997**, *130*, 183. (k) Rosenthal, U.; Pulst, S.; Kempe, R.; Pörschke, K.-R.; Goddard, R.; Proft, B. *Tetrahedron* **1998**, *54*, 1277.

(3) (a) Adams, C. J.; Bruce, M. I.; Horn, E.; Tiekink, E. R. T. *J. Chem. Soc., Dalton Trans.* **1992**, 1157. (b) Adams, C. J.; Bruce, M. I.; Horn, E.; Skelton, B. W.; Tiekink, E. R. T.; White, A. H. *J. Chem. Soc., Dalton Trans.* **1993**, 3299. (c) Choukroun, R.; Donnadieu, B.; Malfant, I.; Haubrich, S.; Frantz, R.; Guerin, C.; Henner, B. *Chem. Commun.* **1997**, 2315. (d) Semmelmann, M.; Fenske, D.; Corrigan, J. F. *J. Chem. Soc., Dalton Trans.* **1998**, 2541. (e) Xu, D.; Hong, B. *Angew. Chem., Int. Ed.* **2000**, *39*, 1826.

(4) (a) Boese, R.; Green, J. R.; Mittendorf, J.; Mohler, D. L.; Vollhardt, K. P. C. *Angew. Chem., Int. Ed. Engl.* **1992**, *31*, 1643. (b) Anderson, H. L.; Faust, R.; Rubin, Y.; Diederich, F. *Angew. Chem., Int. Ed. Engl.* **1994**, *33*, 1366. (c) Anderson, H. L.; Boudon, C.; Diederich, F.; Gisselbrecht, J.-P.; Gross, M.; Seiler, P. *Angew. Chem., Int. Ed. Engl.* **1994**, *33*, 1628. (d) Haley, M. M.; Brand, S. C.; Pak, J. J. *Angew. Chem., Int. Ed. Engl.* **1997**, *36*, 836. (e) Haley, M. M.; Langsdorf, B. L. *Chem. Commun.* **1997**, 1121. (f) Haley, M. M. *Synlett* **1998**, 557. (g) Wan, W. B.; Kimball, D. B.; Haley, M. M. *Tetrahedron Lett.* **1998**, *39*, 6795. (h) Pak, J. J.; Weakley, T. J. R.; Haley, M. M. *J. Am. Chem. Soc.* **1999**, *121*, 8182. (i) Wan, W. B.; Brand, S. C.; Pak, J. J.; Haley, M. M. *Chem. Eur. J.* **2000**, *6*, 2044.

(5) (a) Johnson, B. F. G.; Kakkar, A. K.; Khan, M. S.; Lewis, J.; Dray, A. E.; Friend, R. H.; Wittmann, F. *J. Mater. Chem.* **1991**, *1*, 485. (b) Lewis, J.; Khan, M. S.; Kakkar, A. K.; Johnson, B. F. G.; Marder, T. B.; Fyfe, H. B.; Wittmann, F.; Friend, R. H.; Dray, A. E. *J. Organomet. Chem.* **1992**, *425*, 165.

(6) (a) Brouty, C.; Spinat, P.; Whuler, A. *Acta Crystallogr.* **1980**, *B36*, 2624. (b) Bestmann, H. J.; Hadawi, D.; Behl, H.; Bremer, M.; Hampel, F. *Angew. Chem., Int. Ed. Engl.* **1993**, *32*, 1205. (c) Jiang, W.; Harwell, D. E.; Mortimer, M. D.; Knobler, C. B.; Hawthorne, M. F. *Inorg. Chem.* **1996**, *35*, 4355. (d) Dam, M. A.; Hoogervorst, W. J.; de Kanter, F. J. J.; Bickelhaupt, F.; Spek, A. L. *Organometallics* **1998**, *17*, 1762. (e) Neugebauer, P.; Klingebiel, U.; Noltemeyer, M. *Z. Naturforsch., B* **2000**, *55*, 913. (f) Werz, D. B.; Gleiter, R.; Rominger, F. *J. Am. Chem. Soc.* **2002**, *124*, 10638.

(7) Carré, F.; Dutremez, S. G.; Guérin, C.; Henner, B. J. L.; Jolivet, A.; Tomberli, V.; Dahan, F. *Organometallics* **1999**, *18*, 770.

(8) (a) Baughman, R. H. *J. Polym. Sci., Polym. Phys. Ed.* **1974**, *12*, 1511. (b) Wegner, G. *Pure Appl. Chem.* **1977**, *49*, 443. (c) Baughman, R. H.; Chance, R. R. *Ann. N. Y. Acad. Sci.* **1978**, *313*, 705. (d) Baughman, R. H.; Yee, K. C. *J. Polym. Sci., Macromol. Rev.* **1978**, *13*, 219. (e) Bloor, D. In *Developments in Crystalline Polymers-1*; Bassett, D. C., Ed.; Appl. Sci. Publ.: London, U.K., 1982; p 151. (f) Bloor, D. *Mol. Cryst. Liq. Cryst.* **1983**, *93*, 183. (g) Bloor, D. In *Quantum Chemistry of Polymers−Solid State Aspects*; Ladik, J., André, J. M., Seel, M., Eds.; NATO ASI Series C: Mathematical and Physical Sciences; D. Reidel Publishing Co.: Dordrecht, The Netherlands, 1984; Vol. 123, p 191. (h) Enkelmann, V. *Adv. Polym. Sci.* **1984**, *63*, 91. (i) Cao, G.; Mallouk, T. E. *J. Solid State Chem.* **1991**, *94*, 59.

(9) (a) Corriu, R. J. P.; Guerin, C.; Henner, B.; Jean, A.; Mutin, H. *J. Organomet. Chem.* **1990**, *396*, C35. (b) Corriu, R. J. P.; Gerbier, P.; Guérin, C.; Henner, B. J. L.; Jean, A.; Mutin, P. H. *Organometallics* **1992**, *11*, 2507. (c) Corriu, R.; Gerbier, P.; Guérin, C.; Henner, B. *Angew. Chem., Int. Ed. Engl.* **1992**, *31*, 1195. (d) Corriu, R.; Gerbier, P.; Guérin, C.; Henner, B. *Adv. Mater.* **1993**, *5*, 380. (e) Corriu, R.; Gerbier, P.; Guérin, C.; Henner, B.; Fourcade, R. *J. Organomet. Chem.* **1993**, *449*, 111. (f) Corriu, R.; Gerbier, P.; Guerin, C.; Henner, B. In *Applications of Organometallic Chemistry in the Preparation and Processing of Advanced Materials*; Harrod, J. F., Laine, R. M., Eds.; NATO ASI Series E: Applied Sciences; Kluwer Academic Publishers: The Netherlands, 1995; Vol. 297, p 203. (g) Corriu, R. J. P.; Devylder, N.; Guerin, C.; Henner, B.; Jean, A. *J. Organomet. Chem.* **1996**, *509*, 249. (h) Corriu, R.; Gerbier, P.; Guerin, C.; Henner, B. *Macromol. Symp.* **1996**, *101*, 317. (i) Corriu, R. J. P.; Gerbier, P.; Guérin, C.; Henner, B. *Chem. Mater.* **2000**, *12*, 805. (j) Corriu, R. J. P.; Gerbier, P.; Guérin, C.; Henner, B. *J. Mater. Chem.* **2000**, *10*, 2173.

(10) (a) Baldwin, K. P.; Matzger, A. J.; Scheiman, D. A.; Tessier, C. A.; Vollhardt, K. P. C.; Youngs, W. J. *Synlett* **1995**, 1215. (b) Boese, R.; Matzger, A. J.; Vollhardt, K. P. C. *J. Am. Chem. Soc.* **1997**, *119*, 2052. (c) Guo, L.; Hrabusa, J. M., III; Tessier, C. A.; Youngs, W. J.; Lattimer, R. *J. Organomet. Chem.* **1999**, *578*, 43.

(11) (a) Fomina, L.; Allier, H.; Fomine, S.; Salcedo, R.; Ogawa, T. *Polym. J.* **1995**, *27*, 591. (b) Ogawa, T. *Prog. Polym. Sci.* **1995**, *20*, 943.

(12) (a) Sauteret, C.; Hermann, J.-P.; Frey, R.; Pradère, F.; Ducuing, J.; Baughman, R. H.; Chance, R. R. *Phys. Rev. Lett.* **1976**, *36*, 956. (b) Reinhardt, B. A. *TRIP* **1993**, *1*, 4. (c) Nalwa, H. S. *Adv. Mater.* **1993**, *5*, 341.

Chart 2

$Me_3SiC{\equiv}CC{\equiv}CSiMe_3$ **2a**	$Me_2PhSiC{\equiv}CC{\equiv}CSiPhMe_2$ **2b**
$MePh_2SiC{\equiv}CC{\equiv}CSiPh_2Me$ **2c**	$Ph_3SiC{\equiv}CC{\equiv}CSiPh_3$ **2d**
rac-MePhNpSiC≡CC≡CSiMePhNp **2e**	(*R*,*R*)-(+)-MePhNpSiC≡CC≡CSiMePhNp **2e***
rac-$Ph_3SiC{\equiv}CC{\equiv}CSiMePhNp$ **3**	(*R*)-(+)-$Ph_3SiC{\equiv}CC{\equiv}CSiMePhNp$ **3***
$Me_3SiCH_2C{\equiv}CC{\equiv}CCH_2SiMe_3$ **4a**	$Ph_3SiCH_2C{\equiv}CC{\equiv}CCH_2SiPh_3$ **4b**
$Me_2HSiC{\equiv}CC{\equiv}CSiHMe_2$ **5a**	$Ph_2HSiC{\equiv}CC{\equiv}CSiHPh_2$ **5b**
$Me_3SiC{\equiv}CC{\equiv}CH$ **6a**	$Ph_3SiC{\equiv}CC{\equiv}CH$ **6b**	*rac*-MePhNpSiC≡CC≡CH **6c**
$Me_3SnC{\equiv}CC{\equiv}CSnMe_3$ **7a**	$Ph_3SnC{\equiv}CC{\equiv}CSnPh_3$ **7b**	$Ph_2PC{\equiv}CC{\equiv}CPPh_2$ **8**

Me = methyl; Ph = phenyl; Np = 1-naphthyl

Explicitly, the diacetylenic molecules that have been studied in this work are shown in Chart 2. This series of compounds allows the influence of the following electronic and/or structural variations on polymerization of the C≡CC≡C fragment to be measured:

(i) Change in the nature of the substituents bonded to silicon (see **2a**, **2b**, **2c**, **2d**, **2e**/**2e***, **3**/**3***, **5a**, and **5b**). Such a modification is expected to have a significant impact on the structure and electronics of the resulting polydiacetylenes, similarly to what has been found for diacetylenes bearing aromatic side-groups.[13] Also, as diynes **5a** and **5b** both possess Si−H bonds, it is important to assess the reactivity/inertness of these bonds during polymerization.

(ii) Presence of chiral triorganosilyl groups (see **2e**, **2e***, **3**, and **3***). This aspect is an important one to consider in case the preparation of chiral polydiacetylenes is envisioned.[14] Indeed, incorporation of chiral centers in polydiacetylenes has been used in the past with the hope of getting polymers with high $\chi^{(2)}$ values.[15] Also, it is interesting to assess whether the use of optically active monomers has any effect on the course of the polymerization process and/or induces some kind of organization in the final polymer as compared to when racemic monomers are used. The use of stereogenic silicon centers is anticipated to be difficult to implement with poly[(silylene)diethynylenes)].

(iii) Insertion of a CH_2 spacer between silicon and the triple bonds as in **4a** and **4b**. Numerous purely organic diacetylenes that are known to polymerize in the solid state are dipropargylic compounds, and presumably, this is because the CH_2 groups decrease the steric protection of the triple bonds and confer great flexibility to the diacetylenic molecules. In the case of **4a** and **4b**, the CH_2 bridges should also dampen the influence of the heteroelement on the reactivity of the triple bonds.

(iv) Replacement of one of the SiR_3 groups by a hydrogen atom (compounds **6a**, **6b**, and **6c**). As one end of the C_4 fragment lacks protection, the polymerization mechanism of these diynes might be different from that observed for disubstituted diacetylenes.

(v) Change in the nature of the heteroatom attached to the triple bonds (see **7a**, **7b**, and **8**). This modification might produce greater changes in the polymerization results than those brought about by just changing the substituents borne by the heteroelement.

Scheme 1

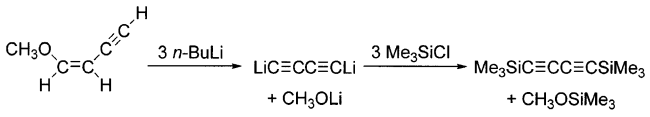

Scheme 2

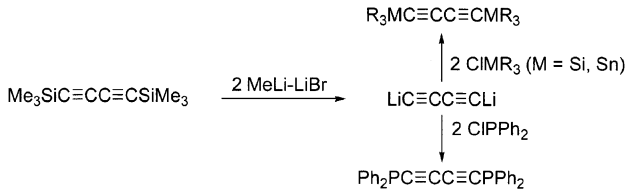

Results and Discussion

1. Syntheses of the Diacetylenic Molecules. 1,4-Bis(trimethylsilyl)buta-1,3-diyne (**2a**) was prepared from (*Z*)-1-methoxybut-1-en-3-yne as reported by Zweifel and Rajagopalan (Scheme 1).[16]

Symmetrical diynes **2b**, **2c**, **2d**, **2e**, **2e***, **5a**, **5b**, **7a**, **7b**, and **8** were synthesized from **2a** as outlined in Scheme 2. This method is more convenient than that presented in Scheme 1, as it avoids the presence of CH_3-OLi in the reaction mixture and, thus, prevents the formation of undesirable byproducts.[7,17,18]

$Me_3SiC{\equiv}CC{\equiv}CH$ (**6a**) is a known compound that is quite readily prepared by monodesilylation of **2a** with

(13) (a) Wegner, G. *J. Polym. Sci., Part B* **1971**, *9*, 133. (b) Orchard, B. J.; Tripathy, S. K. *Macromolecules* **1986**, *19*, 1844. (c) Matsuda, H.; Nakanishi, H.; Kato, S.-I.; Kato, M. *J. Polym. Sci., Part A*: *Polym. Chem.* **1987**, *25*, 1663. (d) Matsuda, H.; Nakanishi, H.; Hosomi, T.; Kato, M. *Macromolecules* **1988**, *21*, 1238. (e) Nakanishi, H.; Matsuda, H.; Okada, S.; Kato, M. *Springer Proc. Phys.* **1988**, *36*, 155. (f) Kim, W. H.; Kodali, N. B.; Kumar, J.; Tripathy, S. K. *Macromolecules* **1994**, *27*, 1819. (g) Coates, G. W.; Dunn, A. R.; Henling, L. M.; Dougherty, D. A.; Grubbs, R. H. *Angew. Chem., Int. Ed. Engl.* **1997**, *36*, 248. (h) Sarkar, A.; Okada, S.; Matsuda, H.; Nakanishi, H. *Chem. Lett.* **1998**, 1073. (i) Sarkar, A.; Okada, S.; Nakanishi, H.; Matsuda, H. *J. Mater. Sci. Lett.* **1998**, *17*, 1449. (j) Sarkar, A.; Talwar, S. S. *J. Chem. Soc., Perkin Trans. 1* **1998**, 4141. (k) Sarkar, A.; Okada, S.; Nakanishi, H.; Matsuda, H. *Macromolecules* **1998**, *31*, 9174. (l) Sarkar, A.; Okada, S.; Matsuzawa, H.; Matsuda, H.; Nakanishi, H. *J. Mater. Chem.* **2000**, *10*, 819.

(14) (a) Drake, A. F.; Udvarhelyi, P.; Ando, D. J.; Bloor, D.; Obhi, J. S.; Mann, S. *Polymer* **1989**, *30*, 1063. (b) Pu, L. *Acta Polym.* **1997**, *48*, 116.

(15) (a) Allan, J. R.; Milburn, G. H. W.; Shand, A. J.; Tsibouklis, J.; Werninck, A. R. In *Organic Materials for Non-Linear Optics*; Hann, R. A., Bloor, D., Eds.; The Royal Society of Chemistry: London, 1989; p 196. (b) Milburn, G. H. W.; Werninck, A.; Tsibouklis, J.; Bolton, E.; Thomson, G.; Shand, A. J. *Polymer* **1989**, *30*, 1004.

(16) Zweifel, G.; Rajagopalan, S. *J. Am. Chem. Soc.* **1985**, *107*, 700.

(17) Bréfort, J. L.; Corriu, R. J. P.; Gerbier, P.; Guérin, C.; Henner, B. J. L.; Jean, A.; Kuhlmann, Th.; Garnier, F.; Yassar, A. *Organometallics* **1992**, *11*, 2500.

(18) Corriu, R. J. P.; Guérin, C.; Henner, B. J. L.; Jolivet, A. *J. Organomet. Chem.* **1997**, *530*, 39.

Scheme 3

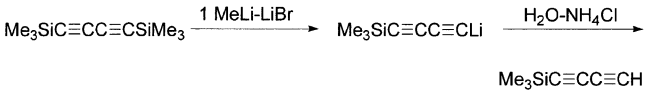

Scheme 4

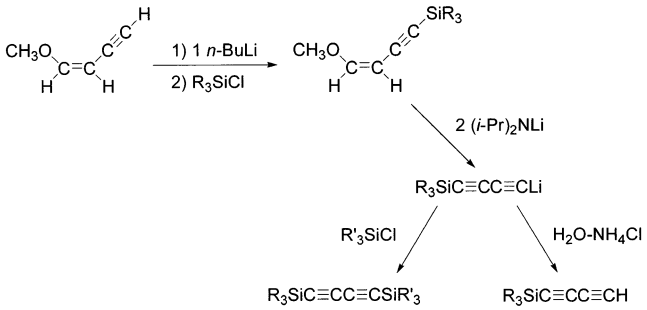

Scheme 5

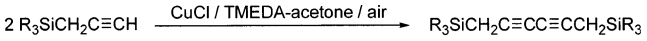

1 equiv of MeLi−LiBr complex, followed by hydrolysis of the intermediate anion (Scheme 3).[19,20]

Diacetylenes **3**, **3***, **6b**, and **6c** were elaborated according to the procedure described in Scheme 4.[7,21,22]

Compounds **4a** and **4b** were synthesized via oxidative dimerization of the parent propargylsilanes under the Hay conditions (Scheme 5).[23]

2. Solid-State Polymerization. 2.1. Crystal Packing Requirements for Diacetylene Polymerization in the Solid State: The Topochemical Principle. A large number of diacetylenic molecules bearing organic substituents have been shown to undergo polymerization in the crystal.[8h,11b] Such polymerization occurs when the following criteria are met (Figure 1): (i) the translational period *d* of the monomer is in the range 4.7−5.2 Å; (ii) R_v is smaller than 4 Å, with a lower limit of 3.4 Å, which represents the van der Waals contact distance of the two rods; (iii) the angle γ between the diacetylene rod and the translational vector is close to 45°. All three geometrical requirements must be met in order to secure a close contact between the C_1 atom of one diacetylene rod and the C_4 atom of the neighboring rod, in the reactive monomer crystal.[8]

The upper limit quoted for $R_{1,4}$ is 5 Å,[8a] but the value for 1,6-bis(9-carbazolyl)-2,4-hexadiyne, 4.22 Å, is the largest value that has been found for a diyne which still shows measurable activity. According to Huntsman,[24] the very low reactivity of the latter compound suggests that the upper limit for $R_{1,4}$ should not be much greater than 4.3 Å. Nevertheless, a few examples have been reported in the literature for which topochemical polymerization was observed, although the aforementioned monomer crystal packing requirements were not met.[24,25] Also, AM1 calculations have proven quite useful to predict the solid-state polymerization activity of diacetylenic molecules.[26]

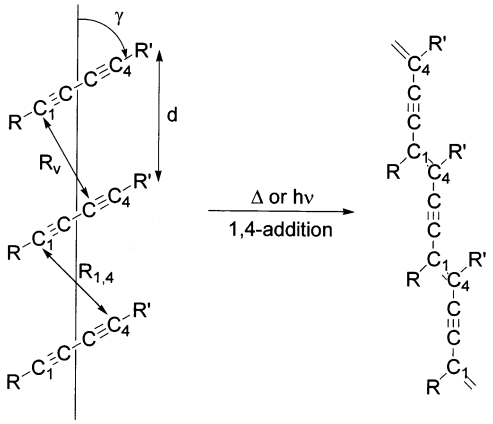

Figure 1. Schematic representation of the topochemical principle for diacetylene polymerization.

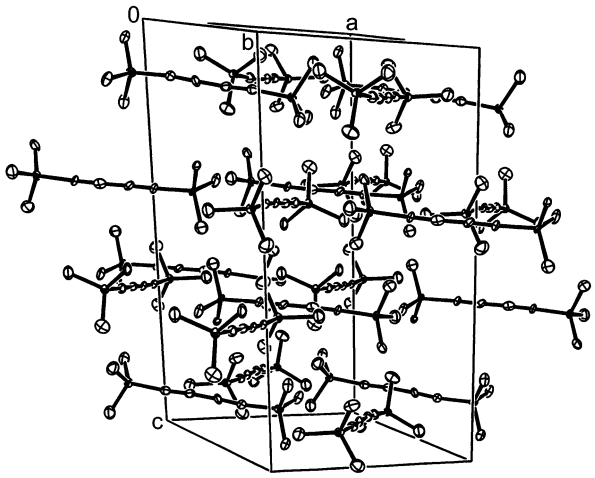

Figure 2. Packing diagram of $Me_3SiC{\equiv}CC{\equiv}CSiMe_3$ (**2a**) at 120 K showing 50% probability ellipsoids. Hydrogen atoms have been omitted for clarity.

2.2. Single-Crystal X-ray Diffraction Studies. $Me_3SiC{\equiv}CC{\equiv}CSiMe_3$ (2a) at 120 K. Although diacetylene **2a** has high symmetry in solution, X-ray crystallography shows that it has no symmetry in the solid. At 120 K, this molecule crystallizes in the triclinic space group $P\bar{1}$ and *Z* is equal to 8 (Table 1).

The compound has a layered structure. The layers are parallel to the *ab* plane and pile up along the *c* direction (Figure 2). Alternately, one layer consists solely of C(11)≡C(12)C(13)≡C(14) and C(31)≡C(32)C(33)≡C(34) fragments and the next one of C(1)≡C(2)C(3)≡C(4) and C(21)≡C(22)C(23)≡C(24) fragments. In each layer, the diacetylenic molecules have the arrangement shown in Figure 3: the C≡CC≡C fragment of one molecule is sandwiched by two $SiMe_3$ groups from neighboring molecules. The C≡CC≡C axes of the neighboring mol-

(19) (a) Holmes, A. B.; Jennings-White, C. L. D.; Schulthess, A. H.; Akinde, B.; Walton, D. R. M. *J. Chem. Soc., Chem. Commun.* **1979**, 840. (b) Holmes, A. B.; Jones, G. E. *Tetrahedron Lett.* **1980**, *21*, 3111.

(20) Bartik, B.; Dembinski, R.; Bartik, T.; Arif, A. M.; Gladysz, J. A. *New J. Chem.* **1997**, *21*, 739.

(21) Stracker, E. C.; Zweifel, G. *Tetrahedron Lett.* **1990**, *31*, 6815.

(22) Brunel, L.; Chaplais, G.; Dutremez, S. G.; Guérin, C.; Henner, B. J. L.; Tomberli, V. *Organometallics* **2000**, *19*, 2516.

(23) (a) Walton, D. R. M.; Waugh, F. *J. Organomet. Chem.* **1972**, *37*, 45. (b) Eastmond, R.; Johnson, T. R.; Walton, D. R. M. *Tetrahedron* **1972**, *28*, 4601. (c) Ghose, B. N. *Synth. React. Inorg. Met.-Org. Chem.* **1994**, *24*, 29. (d) Brandsma, L. *Studies in Organic Chemistry 34*: *Preparative Acetylenic Chemistry*, 2nd ed.; Elsevier: Amsterdam, 1988; p 219.

(24) Huntsman, W. D. In *The chemistry of functional groups, supplement C*: *the chemistry of triple-bonded functional groups Part 2*; Patai, S., Rappoport, Z., Eds.; Wiley: Chichester, U.K., 1983; Chapter 22, pp 917−980.

(25) See refs 1c,d,e,h in ref 10a.

(26) Paley, M. S.; Frazier, D. O.; Abeledeyem, H.; McManus, S. P.; Zutaut, S. E. *J. Am. Chem. Soc.* **1992**, *114*, 3247.

Table 1. Crystal Data and Experimental Details of Data Collection and Refinement for 2a, 2d, 2e*, 4a, and 4b

	2a	2a	2d	2d	2e*	4a	4b
formula	$C_{10}H_{18}Si_2$	$C_{10}H_{18}Si_2$	$C_{40}H_{30}Si_2$	$C_{40}H_{30}Si_2$	$C_{38}H_{30}Si_2$	$C_{12}H_{22}Si_2$	$C_{42}H_{34}Si_2$
fw	194.42	194.42	566.82	566.82	542.80	222.48	594.91
cryst color	colorless	colorless	colorless	colorless	colorless	colorless	colorless
cryst size, mm	0.50 × 0.50 × 0.30	0.45 × 0.35 × 0.15	0.50 × 0.50 × 0.40	0.50 × 0.50 × 0.35	0.50 × 0.20 × 0.03	0.40 × 0.35 × 0.20	0.28 × 0.16 × 0.10
cryst syst	triclinic	monoclinic	triclinic	trigonal	monoclinic	monoclinic	monoclinic
space group	$P\bar{1}$ (No. 2)	$C2/c$ (No. 15)	$P\bar{1}$ (No. 2)	$R\bar{3}$ (No. 148)	$P2_1$ (No. 4)	$C2/m$ (No. 12)	$C2/c$ (No. 15)
a, Å	11.2333(12)	16.2207(13)	14.4203(18)	14.2493(6)	9.573(2)	12.084(3)	24.416(9)
b, Å	11.3336(13)	16.2062(12)	16.814(2)		8.908(4)	7.266(2)	9.458(2)
c, Å	21.969(2)	22.876(2)	19.149(2)	97.340(6)	18.231(4)	9.1776(15)	18.216(8)
α, deg	101.296(13)		113.040(13)				
β, deg	102.676(13)	110.405(14)	108.716(13)		104.80(2)	111.962(15)	130.70(3)
γ, deg	89.885(13)		91.308(15)				
V, Å^3	2673.5(5)	5636.3(9)	3987.6(9)	17116.3(15)	1503.2(7)	747.4(3)	3188.9(26)
Z	8	16	5	21	2	2	4
ρ_{calc}, g cm^{-3}	0.966	0.916	1.180	1.155	1.199	0.989	1.239
F(000)	848	1696	1490	6258	572	244	1256
μ, mm^{-1}	0.223	0.212	0.138	0.135	0.143	0.201	0.1353
temp of data collctn, K	120	203	180	293	293	163	293
graphite-monochromated Mo Kα radiation, Å	0.710 73	0.710 73	0.710 73	0.710 73	0.710 69	0.710 69	0.710 69
$2\theta_{max}$, deg	52.1	52.1	48.4	48.4	49.94	59.92	49.92
no. of reflns collected	26 469	27 401	30 127	41 477	2681	1184	2469
no. of unique reflns	9740	5502	11 787	6136	2530	1137	2415
R_{int} (on I)	0.0308	0.0307	0.0388	0.0417	0.0515	0.0195	0.0683
no. of obsd reflns ($F_o > 4\sigma(F_o)$)	7502	4699	8299	3894	608	850	699
no. of variable params	433	217	946	442	178	48	96
goodness-of-fit on F_o^2 (all reflns)	1.080	0.968	1.214	0.913	0.557	1.022	0.668
w^a	$[\sigma^2(F_o^2) + (0.0383P)^2]^{-1}$	$[\sigma^2(F_o^2) + (0.0306P)^2]^{-1}$	$[\sigma^2(F_o^2) + (0.0207P)^2 + 0.1484P]^{-1}$	$[\sigma^2(F_o^2) + (0.0635P)^2]^{-1}$	$[\sigma^2(F_o^2) + (0.0083P)^2]^{-1}$	$[\sigma^2(F_o^2) + (0.0621P)^2]^{-1}$	$[\sigma^2(F_o^2) + (0.0377P)^2]^{-1}$
max and mean shift/esd	0.001, 0.000	0.001, 0.000	0.001, 0.000	0.002, 0.000	0.000, 0.000	0.000, 0.000	0.000, 0.000
R^b, R_w^c (obsd reflns)	0.0207, 0.0453	0.0228, 0.0476	0.0219, 0.0502	0.0317, 0.0622	0.0467, 0.0565	0.0341, 0.0979	0.0559, 0.1053
R^b, R_w^c (all reflns)	0.0242, 0.0476	0.0238, 0.0477	0.0322, 0.0564	0.0394, 0.0652	0.2916, 0.0744	0.0555, 0.1044	0.2596, 0.1363
largest diff peak and hole, e Å^{-3}	0.24, −0.21	0.30, −0.15	0.11, −0.11	0.15, −0.26	0.22, −0.26	0.39, −0.37	0.37, −0.35

[a] $P = (F_o^2 + 2F_c^2)/3$. [b] $R = \Sigma||F_o| - |F_c||/\Sigma|F_o|$. [c] $R_w = [\Sigma(w(F_o^2 - F_c^2)^2)/\Sigma(w(F_o^2)^2)]^{1/2}$.

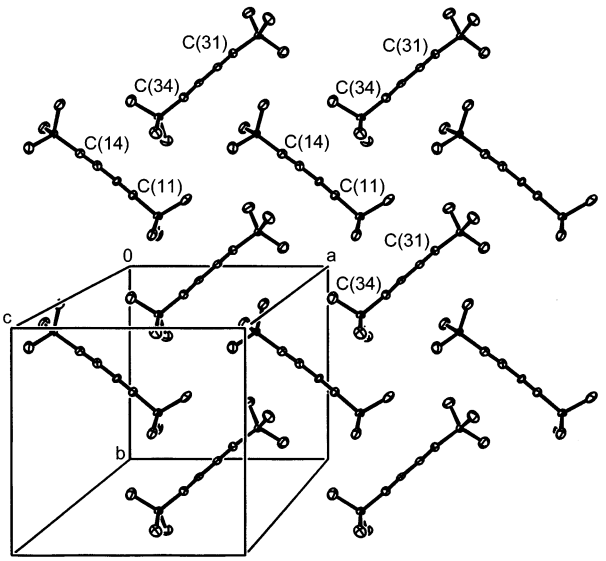

Figure 3. View along the *c* axis of one layer of $Me_3SiC{\equiv}CC{\equiv}CSiMe_3$ (**2a**) at 120 K. Thermal ellipsoids are drawn at the 50% probability level, and hydrogen atoms have been omitted for clarity.

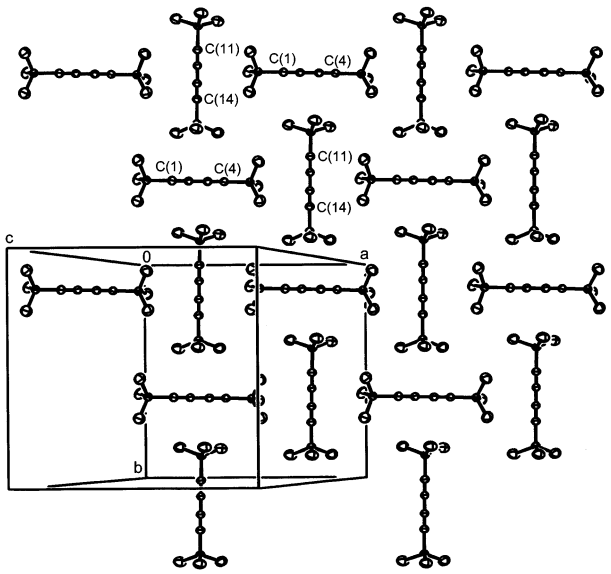

Figure 4. View along the *c* axis of one layer of $Me_3SiC{\equiv}CC{\equiv}CSiMe_3$ (**2a**) at 203 K. Thermal ellipsoids are drawn at the 50% probability level, and hydrogen atoms have been omitted for clarity.

ecules are not perpendicular to the C≡CC≡C axis of the molecule that is sandwiched. Specifically, the angle formed by the least-squares lines[27] through the C(11)≡C(12)C(13)≡C(14) and C(31)≡C(32)C(33)≡C(34) butadiyne units, as calculated by the PARST program,[28] is 81.44°; the angle formed by the least-squares lines through the C(1)≡C(2)C(3)≡C(4) and C(21)≡C(22)C(23)≡C(24) moieties is 81.97°. Looking down the cell along *c*, each layer looks like a grid made of diamonds.

There are 11 intermolecular contacts smaller than 3.8 Å, and only two of them are smaller than 3.5 Å: methyl···methyl = 3.262(2) Å and C_{sp}···methyl = 3.327(2) Å. The two smallest separations between C_{sp} carbons susceptible of getting linked via topochemical polymerization (vide supra) are 5.237(2) and 5.485(1) Å. In the first case, the two diacetylenic rods susceptible of getting linked via topochemical polymerization are rigorously parallel; this results in a single value of 64.4° for the angle γ between the directions of the rods and an axis passing through the centers of these rods. In the second case, the rods are not parallel with each other, and so two different values for the angle γ are found: 50.2° and 55.0°.

$Me_3SiC{\equiv}CC{\equiv}CSiMe_3$ (2a) at 203 K. Several attempts were made to obtain the X-ray structure of **2a** at room temperature using various types of glues and Lindemann capillaries. No data set could be collected in any of these attempts. In only one case did we get cell dimensions that indicated that the crystal system was monoclinic; the values that were found are as follows: $a = 11.508(5)$ Å, $b = 11.589(2)$ Å, $c = 12.317(3)$ Å, $\beta = 118.19(2)°$, $V = 1448(1)$ Å^3. Assuming $Z = 4$, the calculated density is 0.892 g/cm^3. Unfortunately, we were unable to confirm these results by collecting data on other crystals. Currently, it is not clear whether the compound polymerizes in the X-ray beam or something else is going on.

Despite this problem, we were able to collect a full data set and solve the structure of **2a** at 203 K (Table 1). At this temperature, diacetylene **2a** crystallizes in the monoclinic space group *C*2/*c* and *Z* is equal to 16. Here again, the molecule has no symmetry in the solid state. The compound has a layered structure similar to that found in the 120 K X-ray determination (Figure 2): each layer coincides with the *ab* plane and the layers pile up along the *c* direction. The C(1)≡C(2)C(3)≡C(4) and C(11)≡C(12)C(13)≡C(14) fragments are both present in each layer. Their arrangement (Figure 4) is similar to that encountered in the 120 K structure; that is, the C≡CC≡C fragment of one molecule is sandwiched by two $SiMe_3$ groups from neighboring molecules. However, in the 203 K structure, the molecules have undergone a slight rotation in the *ab* plane, and consequently, the C≡CC≡C axes of the neighboring molecules are almost perpendicular to the C≡CC≡C axis of the molecule that is sandwiched. The angle formed by the least-squares lines[27] through the C(1)≡C(2)C(3)≡C(4) and C(11)≡C(12)C(13)≡C(14) butadiyne units, as calculated by the PARST program,[28] is 89.96°. As a result, each layer looks like a grid made of rectangles when looking down the cell along *c*.

Intermolecular contacts are a lot longer and less numerous than those observed in the 120 K structure; only seven contacts are smaller than 3.9 Å: methyl··· methyl = 3.612(4), 3.665(4), 3.738(4), 3.803(4), and 3.857(4) Å and C_{sp}···methyl = 3.836(3) and 3.840(3) Å. The distances between C_{sp} carbons susceptible of getting linked via topochemical polymerization (vide supra) are significantly shorter than those found in the 120 K structure: 4.961(4) and 4.989(4) Å. In the first case, the angle γ between the directions of the diacetylenic rods susceptible of getting linked and an axis passing through the centers of these rods is equal to 51.54°. In the second case, the value of γ is 51.91°.

$Ph_3SiC{\equiv}CC{\equiv}CSiPh_3$ (2d) at 180 K. Similarly to **2a**, diacetylene **2d** has low or no symmetry in the solid state. At 180 K, the latter compound crystallizes in the

(27) Schomaker, V.; Waser, J.; Marsh, R. E.; Bergman, G. *Acta Crystallogr.* **1959**, *12*, 600.
(28) Nardelli, M. *J. Appl. Crystallogr.* **1995**, *28*, 659.

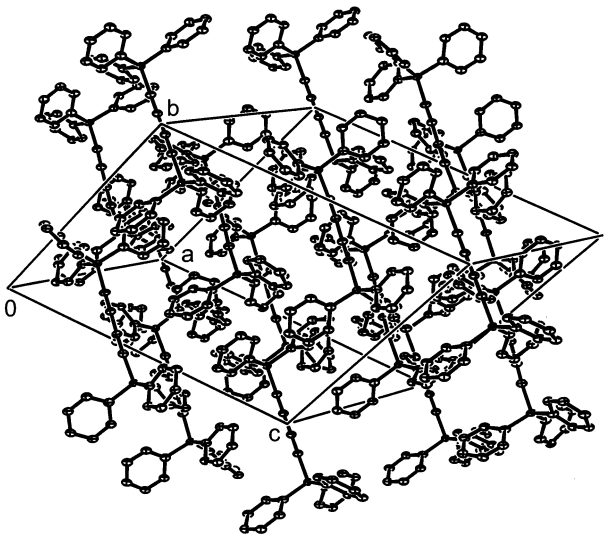

Figure 5. Packing diagram of $Ph_3SiC{\equiv}CC{\equiv}CSiPh_3$ (**2d**) at 180 K showing 30% probability ellipsoids. Hydrogen atoms have been omitted for clarity.

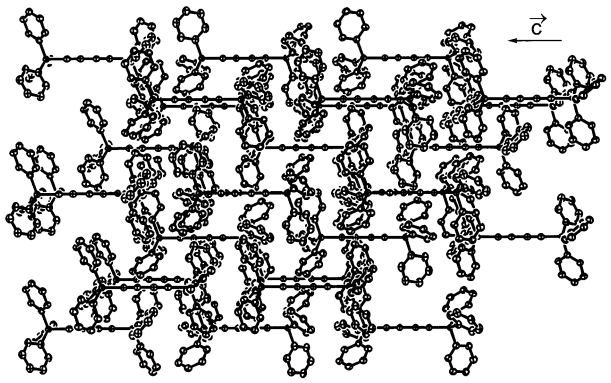

Figure 6. View perpendicular to the *c* axis showing the three-dimensional arrangement of $Ph_3SiC{\equiv}CC{\equiv}CSiPh_3$ (**2d**) at 293 K. Only one-third of the unit cell is depicted. Thermal ellipsoids are drawn at the 30% probability level, and hydrogen atoms have been omitted for clarity.

triclinic space group $P\bar{1}$ and Z is equal to 5 (Table 1): two molecules occupy general positions and one molecule sits on a center of inversion. Unlike **2a**, however, **2d** does not have a layered structure. The three-dimensional arrangement of **2d** (Figure 5) is a compact structure held together by numerous phenyl···phenyl interactions.

There are 20 phenyl···phenyl contacts smaller than 3.7 Å, and three of them are smaller than 3.6 Å: C(18)···C(40) = 3.581(2), C(40)···C(83) = 3.583(2), and C(10)···C(59) = 3.585(2) Å (the atom-labeling scheme is shown in the Supporting Information). The C(18)···C(40) and C(10)···C(59) contacts have a T-shaped geometry, and the C(40)···C(83) interaction is of the parallel displaced type.[29] There is only one short C_{sp}···phenyl distance, namely, C(06)···C(88) = 3.699(2) Å. The smallest separations between C_{sp} carbons susceptible of getting linked via topochemical polymerization (vide supra) are a lot longer than those observed in the X-ray determinations of **2a**, as a result of the steric crowding brought about by the $SiPh_3$ groups. There are four C_{sp}···C_{sp} distances smaller than 8.0 Å: C(05)···C(05′) = 7.692(2), C(04)···C(08) = 7.814(2), C(01)···C(09) = 7.993(2), and C(08)···C(09′) = 7.994(2) Å. In the first case, the two diacetylenic rods susceptible of getting linked via topochemical polymerization are related by a center of inversion; this results in a single value of 60.6° for the angle γ between the directions of the rods and an axis passing through the centers of these rods. In the second case, the rods are not related by any symmetry operation, and so two different values for the angle γ are found: 60.4° and 62.7°.

$Ph_3SiC{\equiv}CC{\equiv}CSiPh_3$ (2d) at 293 K. X-ray crystallography shows that diacetylene **2d** has high symmetry in the solid state at 293 K. At this temperature, the latter compound crystallizes in the trigonal space group $R\bar{3}$ and Z is equal to 21 (Table 1): three molecules sit on a 3-fold rotation axis and one molecule has $\bar{3}$ symmetry. In the room-temperature solid, all of the molecules of **2d** lie parallel to one another, and the molecules are also parallel to the *c* axis (Figure 6).

In this structure, phenyl···phenyl contacts are less numerous but much stronger than those observed in the 180 K determination. There are 13 phenyl···phenyl distances smaller than 3.7 Å, and four of them are smaller than 3.2 Å: C(9)···C(15) = 2.949(2), C(8)···C(14) = 3.083(2), C(9)···C(14) = 3.123(2), and C(8)···C(15) = 3.133(2) Å (see Supporting Information for the atom-labeling scheme). These short distances result from the interaction between the C(7)−C(8)−C(9)−C(10)−C(11)−C(12) and C(13)−C(14)−C(15)−C(16)−C(17)−C(18) phenyl rings: the C(8)−C(9) vector of the first ring intermeshes with the C(14)−C(15) vector of the second ring in a fashion similar to the teeth of two gearwheels whose axes are at 90° to each other. There is no intermolecular contact smaller than 3.7 Å involving a C_{sp} carbon. The smallest separations between C_{sp} carbons susceptible of getting linked via topochemical polymerization (vide supra) are significantly longer than those encountered in the 180 K determination. Intermolecular C_{sp}···C_{sp} distances are all greater than 8.0 Å, and only four of them are smaller than 8.5 Å: C(04)···C(09) = 8.226(2), C(08)···C(012) = 8.253(2), C(01)···C(013) = 8.350(2), and C(05)···C(05′) = 8.394(2) Å. It is worth noting that, because of the 3-fold symmetry of the molecules, each one of these distances has a multiplicity of three, e.g., C(04)···C(09) = C(04)···C(09′) = C(04)···C(09″) = 8.226(2) Å, etc. Furthermore, since all of the molecules lie parallel to one another, only one angle γ between the directions of the rods and an axis passing through the centers of these rods is found for each aforementioned C_{sp}···C_{sp} distance. The values of γ are 64.8°, 61.7°, 57.7°, and 56.5°, respectively.

(*R*,*R*)-(+)-MePhNpSiC≡CC≡CSiMePhNp (2e*). The X-ray crystal structure of **2e*** was determined using data measured at 293 K with Mo Kα radiation (Table 1). This diacetylene crystallizes in the monoclinic space group $P2_1$ and Z is equal to 2. Thus, the molecule has no symmetry. The data were of sufficiently good quality to allow determination of the stereochemistry of the

(29) (a) Cox, E. G.; Cruickshank, D. W. J.; Smith, J. A. S. *Proc. R. Soc. A* (*London*) **1958**, *247*, 1. (b) Burley, S. K.; Petsko, G. A. *Science* (*Washington, D.C.*) **1985**, *229*, 23. (c) Burley, S. K.; Petsko, G. A. *J. Am. Chem. Soc.* **1986**, *108*, 7995. (d) Askew, B.; Ballester, P.; Buhr, C.; Jeong, K. S.; Jones, S.; Parris, K.; Williams, K.; Rebek, J., Jr. *J. Am. Chem. Soc.* **1989**, *111*, 1082. (e) Jorgensen, W. L.; Severance, D. L. *J. Am. Chem. Soc.* **1990**, *112*, 4768. (f) Hunter, C. A.; Sanders, J. K. M. *J. Am. Chem. Soc.* **1990**, *112*, 5525. (g) Hunter, C. A. *Chem. Soc. Rev.* **1994**, *23*, 101. (h) Janiak, C. *J. Chem. Soc., Dalton Trans.* **2000**, 3885. (i) Kim, K. S.; Tarakeshwar, P.; Lee, J. Y. *Chem. Rev.* **2000**, *100*, 4145.

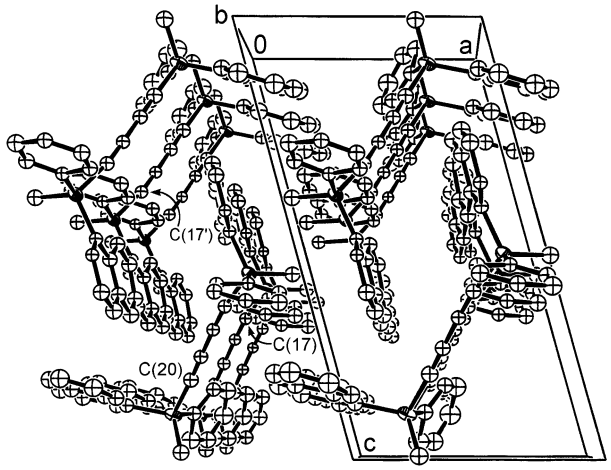

Figure 7. View showing the stacking of the molecules of (*R*,*R*)-(+)-MePhNpSiC≡CC≡CSiMePhNp (**2e***) in the *b* direction. Thermal ellipsoids are drawn at the 30% probability level, and hydrogen atoms have been omitted for clarity.

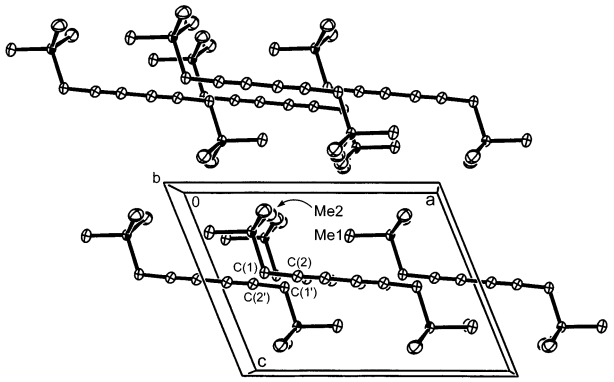

Figure 8. Packing diagram of $Me_3SiCH_2C{\equiv}CC{\equiv}CCH_2SiMe_3$ (**4a**) viewed down *b*. Thermal ellipsoids are drawn at the 50% probability level, and hydrogen atoms have been omitted for clarity.

silicon centers: it is *R* in both cases. Looking at the cell in the *b* direction (Figure 7), one can see stacks of diacetylenic molecules; the stacks are parallel to one another. In each stack, two consecutive molecules are separated by a distance equal to *b* (8.908(4) Å).

There are 16 intermolecular contacts smaller than 3.7 Å, and only five of them are smaller than 3.65 Å: 3.561(14), 3.599(14), 3.603(15), 3.626(15), and 3.635(15) Å. These five contacts each involve a phenyl group and a naphthyl group. The shortest intermolecular contact involving a C_{sp} carbon, C(6)···C(17), is 3.678(14) Å, and the shortest contact involving a methyl group, Me2···C(23), is 3.691(16) Å (the atom-labeling scheme is shown in the Supporting Information). The smallest intermolecular distance between C_{sp} carbons susceptible of getting linked via topochemical polymerization (vide supra) is 7.904(17) Å. This distance corresponds to the separation between the C(17) carbon of one diacetylenic molecule and the C(20) atom of the next molecule located just above the first one in the same stack. The angle γ between the directions of the C_4 rods and an axis passing through the centers of these rods is equal to 62.4°. The next smallest intermolecular distance between C_{sp} carbons susceptible of getting linked via topochemical polymerization is 7.918(15) Å. This distance corresponds to the separation between the C(17) carbon of one diacetylenic molecule with coordinates (*x*, *y*, *z*) and the C(17′) atom of a second molecule with coordinates (1−*x*, 1/2+*y*, 1−*z*) located in an adjacent stack (the two molecules are related by a 2-fold screw axis). In this case, the angle γ between the directions of the C_4 rods and an axis passing through the centers of these rods is equal to 69.3°.

$Me_3SiCH_2C{\equiv}CC{\equiv}CCH_2SiMe_3$ (4a). The X-ray crystal structure of **4a** was determined at 163 K (Table 1). This diacetylene crystallizes in the monoclinic space group *C*2/*m* and *Z* is equal to 2. The molecule occupies a 2/*m* special position. Only one-fourth of the molecule is crystallographically unique. The compound has a layered structure. Each layer coincides with the *ac* plane and contains the diacetylenic fragment, the methylene groups, the silicon atoms, and two methyl groups. The remaining methyl groups on each silicon stick above and below this plane. The layers pile up along the *b* direction, and the interlayer distance is *b*/2. Looking at the cell in the *b* direction (Figure 8), one can see series of $CH_2C{\equiv}CC{\equiv}CCH_2$ moieties that give the impression of being aligned along an axis. However, in this view, two consecutive $CH_2C{\equiv}CC{\equiv}CCH_2$ fragments do not belong to the same plane.

The rods are separated by layers of $SiMe_3$ groups in the *c* direction. The inter-rod distance is equal to *c*, i.e., 9.1776(15) Å. The closest contacts between two neighboring molecules involve methylene groups: C(1)···C(1′) = 3.739(1) Å and C(1)···C(2′) = 3.751(1) Å. There are two short intermolecular contacts involving methyl groups: Me1···C(1′) = 3.814(3) Å and Me2···C(2′) = 3.846(2) Å. The shortest CH_3···CH_3 distances span the range 4.015(3)−4.199(3) Å, and there are five of them. The smallest intermolecular separation between C_{sp} carbons susceptible of getting linked via topochemical polymerization, C(2)···C(2′), is 4.292(2) Å. An axis passing through the midpoints of the central C_{sp}−C_{sp} single bonds of the diacetylenic molecules containing C(2) and C(2′) would make an angle γ of 31.3° with the C≡CC≡C segment of each molecule.

$Ph_3SiCH_2C{\equiv}CC{\equiv}CCH_2SiPh_3$ (4b). The X-ray crystal structure of **4b** was determined at 293 K (Table 1). This diacetylene crystallizes in the monoclinic space group *C*2/*c* and *Z* is equal to 4. The molecule lies on a 2-fold axis of symmetry. Only one-half of the molecule is crystallographically unique. Looking at the cell in the *b* direction (Figure 9), one can see parallel stacks of diacetylenic molecules that are almost perpendicular to the *c* axis. In each stack, two consecutive molecules are separated by a distance equal to *b* (9.458(2) Å).

The shortest CH_2···C_{arom} contacts are 3.794(8), 3.872(10), and 3.878(9) Å. The shortest C(2)···C_{arom} distances are 3.925(10), 3.987(9), and 4.019(9) Å (C(2) is the C_{sp} carbon directly attached to the CH_2 group). The shortest C(3)···C_{arom} contacts are 3.785(9), 3.844(9), 3.985(9), and 4.016(9) Å (C(3) is the C_{sp} carbon in β-position to the CH_2 group). C_{arom}···C_{arom} separations are a lot shorter and more numerous than the aforementioned distances and seem to be responsible for the cohesion of the crystal. There are four short C_{arom}···C_{arom} contacts: 3.582(9), 3.634(12), 3.645(10), and 3.650(9) Å; three of them are of the edge-to-face type and one of them is of the parallel displaced type.[29] The next shortest C_{arom}···C_{arom} distances are in the range 3.737(10)−3.782(9) Å,

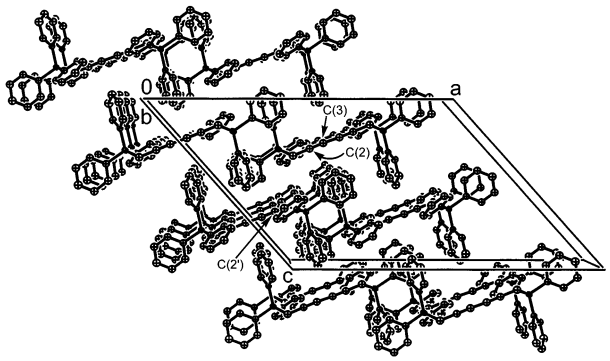

Figure 9. View showing the stacking of the molecules of $Ph_3SiCH_2C{\equiv}CC{\equiv}CCH_2SiPh_3$ (**4b**) in the *b* direction. Thermal ellipsoids are drawn at the 50% probability level, and hydrogen atoms have been omitted for clarity.

and there are eight of them. The three smallest intermolecular distances between C_{sp} carbons susceptible of getting linked via topochemical polymerization are 7.150, 8.416, and 8.747 Å. The 7.150 Å distance corresponds to the separation between the C(2) carbon of one diacetylenic molecule with coordinates (*x*, *y*, *z*) and the C(2′) atom of a second molecule with coordinates (1/2−*x*, 1/2−*y*, 2−*z*) located in an adjacent stack. An axis passing through the midpoints of the central $C_{sp}-C_{sp}$ single bonds of these two molecules would make an angle γ of 33.3° with the C≡C segments of each molecule.

Last, low-temperature differential scanning calorimetry (DSC) studies (down to −120 °C) have been carried out on **2a** and **2d** that corroborate the phase changes observed by X-ray diffraction: a sharp reversible endotherm was observed at −88.4 °C in the case of **2a** (ΔH = 12.36 J/g). A broad reversible endotherm was observed at −24.9 °C in the case of **2d** (ΔH = 2.84 J/g).

2.3. Solid-State Polymerization Experiments. X-ray crystallographic studies on **2d**, **2e***, and **4b** (vide supra) show that the smallest $R_{1,4}$ distances in these compounds are in the range 7.150−8.226 Å. The X-ray crystal structure of **3*** has been reported by us.[7] This compound gives a 1:1 host−guest complex upon crystallization from dioxane. In this clathrate, the smallest distances between possibly reacting terminal acetylenic carbon atoms in neighboring molecules are 7.764(8) and 7.809(12) Å. The shortest intermolecular contacts between the extremities of neighboring diacetylenic rods are 9.590 and 9.830 Å in $Ph_3SnC{\equiv}CC{\equiv}CSnPh_3{\cdot}CHCl_3$[6a] and 9.660 and 9.904 Å in $Ph_3SnC{\equiv}CC{\equiv}CSnPh_3{\cdot}$dioxane,[7] and these distances span the range 7.981(4)−8.569(5) Å for unsolvated $Ph_3SnC{\equiv}CC{\equiv}CSnPh_3$.[7] All of these values are much too large to expect topochemical polymerization, and, in agreement with this, **2e*** showed no polymerization reactivity upon irradiation with a 100 krad dose of γ-rays or heating to 150 °C, in air, for 66 h.

$Me_3SiC{\equiv}CC{\equiv}CSiMe_3$ (**2a**) and $Me_3SiCH_2C{\equiv}CC{\equiv}CCH_2SiMe_3$ (**4a**) seemed to be better candidates for solid-state polymerization studies: the $R_{1,4}$ distances found for **2a** (4.961(4)−5.485(1) Å) are close to the upper limit for solid-state polymerization (5 Å) quoted by Baughman,[8a] and that found for **4a** (4.292(2) Å) is just below the 4.3 Å limit given by Huntsman.[24] Some of the γ angles found in the X-ray crystal structures of **2a** and **4a** differ significantly from the needed 45° value, but deviations as large as 15° from the optimum 45° angle have been observed for diacetylenes that showed polymerization activity.[24] With this in mind, both diacetylenes were irradiated at room temperature with a 100 krad dose; no polymerization activity was detected with either compound based on the absence of color change and the lack of change in the IR spectrum.

Diacetylene **6c** was also tested for solid-state polymerization activity. The X-ray crystal structure of **6c** is not known but, as one end of the C_4 rod is lacking steric protection, one might expect this diacetylene to be reactive. In a first experiment, diyne **6c** was irradiated at room temperature with a 100 krad dose. No appreciable color change of the powder was observed and no change was noticed in the IR spectrum, indicating that polymerization had not taken place. In a second experiment, **6c** was heated to 70 °C for 13 days. Interestingly, slow polymerization of this diacetylene was observed. Integration of the DSC curve gives a heat of polymerization of −195 cal/g (−57.7 kcal/mol). This value is somewhat larger than the heats of polymerization (around −36 kcal/mol) reported for hexa-2,4-diynylene bis(*p*-toluenesulfonate) (PTS) and 1,6-bis(2,4-dinitrophenoxy)-2,4-hexadiyne (DNP).[30−32] An analysis of the polymeric material by infrared spectroscopy showed a band at 2154 cm^{-1} characteristic of an enyne structure (vide infra). Since this band is the same as that observed in the infrared spectrum of the molten-state polymerized material (see below), we believe that a 1,2-addition process has taken place in the solid-state polymerization experiment. The dichotomy between the irradiation results of **6c** and the thermal polymerization results may be rationalized as follows: in the UV spectrum of a crystal of dodeca-5,7-diynylene bis[((*n*-butoxycarbonyl)methyl)urethane] (4BCMU), the C_4 fragment absorbs weakly between 270 and 290 nm. The extinction coefficient at 270 nm is about 40 L mol^{-1} cm^{-1}. On the other hand, naphthalene and methylnaphthalenes exhibit strong absorptions in that region with extinction coefficients of about 5000 L mol^{-1} cm^{-1}. Consequently, at 270 nm, over 99% of the incoming photons are absorbed by the naphthyl group. In addition, as naphthalene absorbs up to 320 nm, energy transfer from the diacetylenic fragment to the naphthyl group is easy. All of these factors concur to prevent photochemical polymerization from occurring.

Since attempts to polymerize our compounds in the solid state proved rather disappointing, a study of the polymerization of these molecules in the molten state was undertaken, as previously reported for several purely organic diacetylenic systems.[11]

3. Molten-State Polymerization. 3.1. DSC Studies. DSC analyses were carried out on diacetylenes **2**−**8** to determine the temperature at which polymerization takes place. The results are summarized in Table 2.

Table 2 shows that polymerization occurs after the compounds have melted. In the case of disilylated diacetylenes **2a**, **2b**, **2c**, **2e**, **2e***, **3**, **3***, and **5b**, polym-

(30) Chance, R. R.; Patel, G. N.; Turi, E. A.; Khanna, Y. P. *J. Am. Chem. Soc.* **1978**, *100*, 1307.
(31) Bertault, M.; Schott, M.; Brienne, M. J.; Collet, A. *Chem. Phys.* **1984**, *85*, 481.
(32) Kalyanaraman, P. S.; Garito, A. F.; McGhie, A. R.; Desai, K. N. *Makromol. Chem.* **1979**, *180*, 1393.

Table 2. DSC Results for Compounds 2−8[a]

compound	endotherm,[b] °C	exotherm[c] T_o, °C	exotherm[c] T_{max}, °C
$Me_3SiC{\equiv}CC{\equiv}CSiMe_3$ (**2a**)[d]	110.5	270	340
$Me_2PhSiC{\equiv}CC{\equiv}CSiPhMe_2$ (**2b**)	69.2	290	333
$MePh_2SiC{\equiv}CC{\equiv}CSiPh_2Me$ (**2c**)	143.2	322	350
$Ph_3SiC{\equiv}CC{\equiv}CSiPh_3$ (**2d**)	302.4	330	387
rac-MePhNpSiC≡CC≡CSiMePhNp (**2e**)	several between 100 and 190	290	348
(*R*,*R*)-(+)-MePhNpSiC≡CC≡CSiMePhNp (**2e***)	179.5	290	347
rac-$Ph_3SiC{\equiv}CC{\equiv}CSiMePhNp$ (**3**)	146.3 155.7	310	360
(*R*)-(+)-$Ph_3SiC{\equiv}CC{\equiv}CSiMePhNp$ (**3***)	166.3	305	363
$Me_3SiCH_2C{\equiv}CC{\equiv}CCH_2SiMe_3$ (**4a**)	47.8	[e]	
$Ph_3SiCH_2C{\equiv}CC{\equiv}CCH_2SiPh_3$ (**4b**)	208.1	255	300
$Me_2HSiC{\equiv}CC{\equiv}CSiHMe_2$ (**5a**)	[f]		
$Ph_2HSiC{\equiv}CC{\equiv}CSiHPh_2$ (**5b**)	93.4	200	244.4
$Me_3SiC{\equiv}CC{\equiv}CH$ (**6a**)	[g]	80	133
$Ph_3SiC{\equiv}CC{\equiv}CH$ (**6b**)	117	117	125
rac-MePhNpSiC≡CC≡CH (**6c**)	96.1	96.1	109.2
$Me_3SnC{\equiv}CC{\equiv}CSnMe_3$ (**7a**)	137.9	194[h]	235[h]
$Ph_3SnC{\equiv}CC{\equiv}CSnPh_3$ (**7b**)	245	245	255
$Ph_2PC{\equiv}CC{\equiv}CPPh_2$ (**8**)	109	140	182

[a] Experiments carried out under a dinitrogen flow, with a heating rate of 5 °C/min. [b] Corresponds to melting. [c] Corresponds to polymerization of the triple bonds. T_o, onset temperature; T_{max}, temperature at the maximum of the exotherm. [d] Vaporizes at 234.3 °C. The DSC analysis was performed with a pressure-proof crucible. [e] Vaporizes before polymerization takes place (bp 263.9 °C). [f] Not studied. bp: 63.5 °C/3 mm. [g] Liquid at room temperature. [h] A second exotherm (T_o = 300 °C; T_{max} = 330 °C) is observed after that due to polymerization that presumably corresponds to degradation of the polymer.

erization starts between 100 and 220 degrees after melting. As far as **2d** is concerned, a 30 degree difference is observed between melting and polymerization. Terminal diacetylenes **6b** and **6c** behave differently: polymerization starts as soon as melting has begun.

Also evident from Table 2 is the fact that the polymerization temperature is strongly influenced by the nature of the substituents borne by the silicon atoms and, especially, by the steric bulk of these substituents. For symmetrical diynes **2a**−**2e*** and **5b**, the temperature at which polymerization starts decreases in the order Ph_3Si > $MePh_2Si$ > Me_2PhSi, MePhNpSi > Me_3Si > Ph_2HSi. This sequence parallels the $R_{1,4}$ distances found by X-ray diffraction. The same variation is observed for monosilylated diacetylenes **6a**−**6c**, i.e., **6b** > **6c** > **6a**, although the polymerization mechanism is different in this case (see section 3.4). Finally, as might be intuitively expected, the polymerization temperatures of unsymmetrical diynes **3** and **3*** lie between those of symmetrically substituted diacetylenes **2e** and **2e*** and that of **2d**.

The DSC results concerning racemic mixtures **2e** and **3** call for further comments: these compounds show two or more endotherms before polymerization takes place. This contrasts with the thermal behavior of the pure enantiomers **2e*** and **3***, which each exhibit a single melting endotherm. Several reasons can be put forth to explain this dichotomy: in the case of **2e**, three diastereoisomers (two enantiomers and one meso compound) are possible that can lead to two separate endotherms. Diacetylene **3** does not have that problem, as it consists of only two enantiomers. Another important aspect to consider is whether these mixtures of optical isomers crystallize as conglomerates or racemates or assemble into more complicated crystalline structures. In principle, these various crystalline forms should give rise to separate endotherms. Last, problems due to polymorphism and/or desolvation of clathrates upon drying are possible: we have found that various samples of **2e**, which were crystallized under different conditions, gave DSC curves that did not show the same number of endotherms. Furthermore, **3*** has been reported to give a 1:1 host−guest complex with dioxane that readily desolvates on standing at room temperature.[7]

The polymerization temperatures of **4b** (255 °C), **7b** (245 °C), and **8** (140 °C) are significantly lower than that of **2d** (330 °C). In the case of **4b**, this difference is easily accounted for by the presence of two CH_2 spacers that diminish the steric protection brought about by the bulky $SiPh_3$ groups, so the C_4 rod is more accessible to neighboring diacetylene units. The same reasoning is likely to be true for **8**, as phosphorus is only three-coordinate and, thus, a lesser degree of steric shielding is provided to the reacting triple bonds. But, because phosphorus and silicon have dissimilar electronegativities (2.1 for phosphorus and 1.8 for silicon),[33] electronic effects may also contribute to the observed difference. Considering that tin is four-coordinate and has a larger covalent radius than silicon (1.41 Å for tin and 1.18 Å for silicon),[33] one could expect the polymerization temperature of **7b** to be higher than that of **2d**. Experimentally, the opposite trend is observed, which seems to suggest that steric arguments should be ruled out. Also, electronic effects cannot account for this difference, as silicon and tin have identical Pauling electronegativities.[33] Nonetheless, this observation seems to be general, as the same large difference in polymerization temperature exists between **7a** (194 °C) and **2a** (270 °C).

3.2. Polymerization Studies of $R_3SiC{\equiv}CC{\equiv}CSiR_3$, $R_3SnC{\equiv}CC{\equiv}CSnR_3$, and $Ph_2PC{\equiv}CC{\equiv}CPPh_2$. The molten-state polymerization conditions and results are summarized in Table 3. Only in the case of **7b** was the experiment carried out in the solid state because problems due to decomposition were encountered at the melting temperature.

(33) Greenwood, N. N.; Earnshaw, A. *Chemistry of the Elements*; Pergamon: Oxford, U.K., 1984.

Table 3. Experimental Conditions and Results of Molten-State Polymerization Studies on Diacetylenes 2−8[a]

compound	temperature, °C	time	infrared results
$Me_3SiC{\equiv}CC{\equiv}CSiMe_3$ (**2a**)	235	28 days	enyne + triene
$Ph_3SiC{\equiv}CC{\equiv}CSiPh_3$ (**2d**)[b]	300	1 day	enyne
rac-MePhNpSiC≡CC≡CSiMePhNp (**2e**)	235	7 days	enyne + triene
(*R*,*R*)-(+)-MePhNpSiC≡CC≡CSiMePhNp (**2e***)	235	10 days	enyne + triene
(*R*)-(+)-$Ph_3SiC{\equiv}CC{\equiv}CSiMePhNp$ (**3***)	235	11 days	enyne + triene
$Me_3SiCH_2C{\equiv}CC{\equiv}CCH_2SiMe_3$ (**4a**)	235	4 days	polyaromatic
$Ph_3SiCH_2C{\equiv}CC{\equiv}CCH_2SiPh_3$ (**4b**)	235	24 h	polyaromatic
$Me_2HSiC{\equiv}CC{\equiv}CSiHMe_2$ (**5a**)	200	5 h	enyne + triene + Si−H
$Me_2HSiC{\equiv}CC{\equiv}CSiHMe_2$ (**5a**)	400	5 h	enyne + triene
$Ph_2HSiC{\equiv}CC{\equiv}CSiHPh_2$ (**5b**)	300	5 h	enyne + triene + Si−H
$Me_3SiC{\equiv}CC{\equiv}CH$ (**6a**)	50	6 h	enynes + **6a**
$Me_3SiC{\equiv}CC{\equiv}CH$ (**6a**)	110	2 h	enyne + triene
$Ph_3SiC{\equiv}CC{\equiv}CH$ (**6b**)	115	1 h	enyne
rac-MePhNpSiC≡CC≡CH (**6c**)	109	30 min	enyne
$Me_3SnC{\equiv}CC{\equiv}CSnMe_3$ (**7a**)	170	10 h	enyne + triene
$Ph_3SnC{\equiv}CC{\equiv}CSnPh_3$ (**7b**)	200	5 h	enyne + triene
$Ph_3SnC{\equiv}CC{\equiv}CSnPh_3$ (**7b**)	225	5 h	enyne + triene + Ph_4Sn
$Ph_2PC{\equiv}CC{\equiv}CPPh_2$ (**8**)	180	2 h	enyne

[a] The polymerization process of tin-containing diyne **7b** was studied in the solid state because problems due to decomposition were encountered at the melting temperature. [b] No polymerization was observed upon heating **2d** to 235 °C for 28 days.

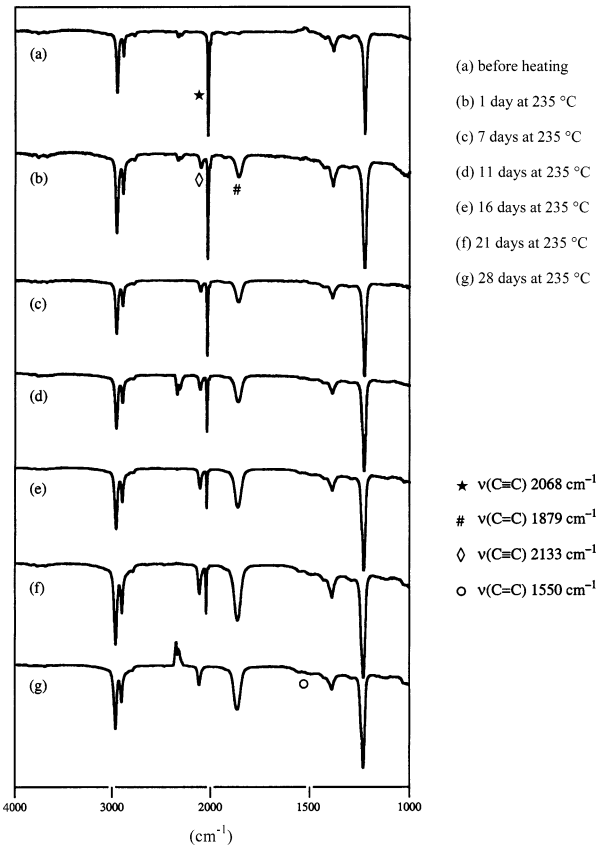

Figure 10. IR monitoring of the polymerization reaction of $Me_3SiC{\equiv}CC{\equiv}CSiMe_3$ (**2a**).

Molten-state polymerization of $Me_3SiC{\equiv}CC{\equiv}CSiMe_3$ (**2a**) was carried out at 235 °C for 28 days. A dark powder with a metallic luster was recovered at the end of the heating period. Figure 10 shows the IR spectrum of the reaction mixture at various times during the experiment and Figure 10g the spectrum of the final solid. In the C≡C stretching region, the band due to starting diyne **2a** (2068 cm^{-1}) is no longer present and a new vibration has appeared at 2133 cm^{-1} that corresponds to the $\nu_{C\equiv C}$ of enyne units. A weak band is also detected at 1550 cm^{-1} that is assigned to the $\nu_{C=C}$ of enyne units. A third new band is visible at 1879 cm^{-1} that corresponds to the $\nu_{C=C}$ of a triene skeleton.[9a,b] Interestingly, the enyne structure and the butatriene skeleton both form in significant amounts right after the experiment has begun (Figure 10b). As polymerization proceeds, the amount of butatriene motifs increases more rapidly than the amount of enyne motifs.

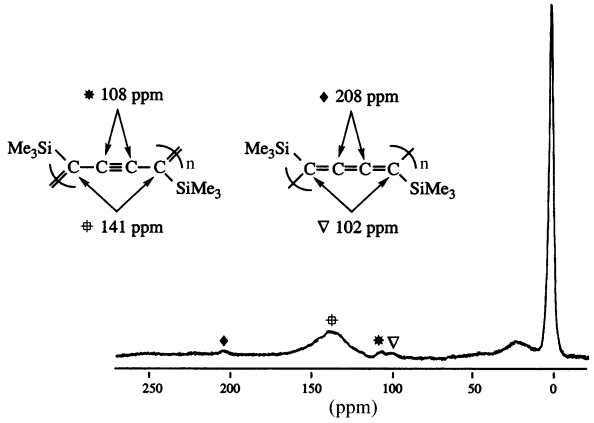

Figure 11. CP/MAS ^{13}C NMR spectrum of poly-**2a**: observation frequency 100.6 MHz, number of transients 34 106, recycle delay time 10 s, contact time 5 ms, 0 Hz line broadening, spinning rate 12 kHz.

The presence of enyne and triene structures in the final solid was confirmed by solid-state ^{13}C NMR measurements (Figure 11): the signals at 108 and 141 ppm are assigned to carbons from enyne units and those at 102 and 208 ppm to carbons from triene units. The solid-state ^{29}Si NMR spectrum shows four resonances at −18.9, −9.2, −3.4, and +1.9 ppm, corresponding to $SiMe_3$ groups in different environments.

A MALDI-TOF mass spectrometric analysis was carried out on poly-**2a** to determine the size of the polymer chain (Figure 12). This analysis shows that poly-**2a** consists of a mixture of oligomers with four to seven repeat units (see Table 4). The 4*M* peak is the most intense peak in the spectrum, and a monotonic decrease in peak intensity is observed on passing from the 4*M* to the 7*M* oligomer. Also, some additional peaks due to $SiMe_3$ loss are observed (Figure 12).

A dark powder with a metallic luster resulted from the heating of **2e** to 235 °C for 7 days (see Table 3). IR

Table 4. Summary of MALDI-TOF MS Results

diacetylenic monomer	observed oligomers (relative intensity)[a]
$Me_3SiC{\equiv}CC{\equiv}CSiMe_3$ (**2a**)	4*M* (0.12), 5*M* (0.09), 6*M* (0.04), 7*M* (0.02)
$Ph_3SiC{\equiv}CC{\equiv}CSiPh_3$ (**2d**)	[b]
rac-MePhNpSiC≡CC≡CSiMePhNp (**2e**)	2*M* (0.14), 3*M* (0.08), 4*M* (0.04), 5*M* (0.02)
(*R*,*R*)−(+)-MePhNpSiC≡CC≡CSiMePhNp (**2e***)	2*M* (0.062), 3*M* (0.026), 4*M* (0.014)
(*R*)−(+)-$Ph_3SiC{\equiv}CC{\equiv}CSiMePhNp$ (**3***)	2*M* (0.11), 3*M* (0.05), 4*M* (0.03)
$Me_3SiCH_2C{\equiv}CC{\equiv}CCH_2SiMe_3$ (**4a**)	3*M* (0.14), 4*M* (0.08), 5*M* (0.07), 6*M* (0.06), 7*M* (0.03), 8*M* (0.02)
$Ph_3SiCH_2C{\equiv}CC{\equiv}CCH_2SiPh_3$ (**4b**)	2*M* (0.037), 3*M* (0.059), 4*M* (0.014)
rac-MePhNpSiC≡CC≡CH (**6c**)	3*M* (0.087), 4*M* (0.026), 5*M* (0.032), 6*M* (0.035), 7*M* (0.031), 8*M* (0.028), 9*M* (0.025), 10*M* (0.022)

[a] *M* = molecular weight of the diacetylenic monomer. [b] No exploitable results were obtained.

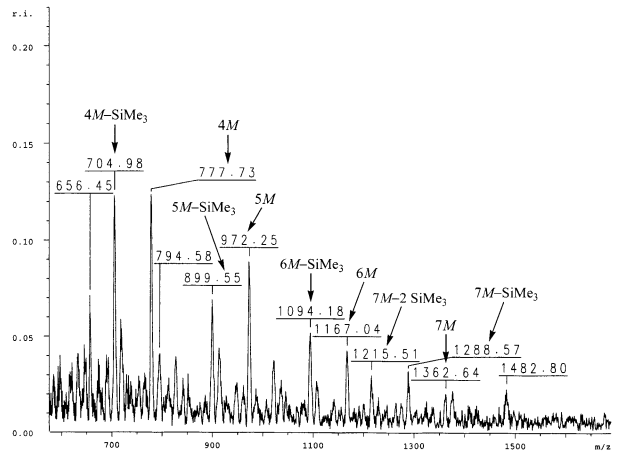

Figure 12. MALDI-TOF mass spectrum of poly-**2a**.

monitoring of the polymerization reaction showed the disappearance of the $\nu_{C\equiv C}$ of **2e** (2069 cm^{-1}) and the growth of two new vibrations at 2115 and 1886 cm^{-1}. These new bands correspond to the $\nu_{C\equiv C}$ of enyne motifs and to the $\nu_{C=C}$ of triene motifs. At the beginning of the experiment, the C═C stretching band of the triene units is more intense than the C≡C stretching band of the enyne units, and the former vibration reaches a maximum intensity after a heating period of about 1 day. As heating is continued, the intensity of the C═C stretching band of the triene units decreases and the intensity of the C≡C stretching band of the enyne units increases. Solid-state ^{13}C NMR measurements confirmed the IR results obtained on the final solid: two weak peaks were observed at 100 and 110 ppm that are assigned to the sp^2 carbons of a butatriene structure and to the sp carbons of an enyne structure, respectively. The sp^2 carbons of the enyne structure appear as a small hump at 148 ppm at the base of the aromatic signals. The solid-state ^{29}Si NMR spectrum consists of a broad envelope in which five resonances can be clearly identified (δ = −28.0, −23.1, −14.3, −9.1, and −1.0 ppm). Oligomers with two to five repeat units were observed in the MALDI-TOF mass spectrum of poly-**2e** (Table 4).

Diacetylene **2e*** was heated to 235 °C for 10 days (see Table 3). No obvious difference was noticed in the IR and solid-state NMR results between poly-**2e*** and poly-**2e**. Also, oligomers with similar sizes were observed by MALDI-TOF mass spectrometry (Table 4).

Diyne **3*** was heated to 235 °C for 11 days (see Table 3). IR monitoring of the polymerization process showed the disappearance of the $\nu_{C\equiv C}$ of **3*** (2069 cm^{-1}) and the growth of two new vibrations at 2140 and 1886 cm^{-1}. These new bands correspond to the $\nu_{C\equiv C}$ of enyne motifs and to the $\nu_{C=C}$ of triene motifs. As observed during the polymerization of **2e** and **2e***, the C═C stretching band of the triene units is more intense than the C≡C stretching band of the enyne units at the beginning of the experiment. However, unlike poly-**2e** and poly-**2e***, the $\nu_{C=C}$ of the triene units does not grow as quickly and reaches a maximum intensity after a heating period of 8 to 9 days. Near the end of the heating period, the intensity of the C═C stretching band of the triene units decreases, whereas that of the C≡C stretching band of the enyne units stabilizes at some maximum. Solid-state ^{13}C NMR measurements agree with the IR results obtained on the final solid: two weak peaks were observed at 106 and 112 ppm that are assigned to the sp^2 carbons of a butatriene structure and to the sp carbons of an enyne structure, respectively. The sp^2 carbons of the enyne structure appear as a small hump at 151 ppm at the base of the aromatic signals. The sp carbons of the triene structure show up as a very small signal at 222 ppm. The solid-state ^{29}Si NMR spectrum consists of a broad envelope in which five resonances can be clearly identified (δ = −29.2, −18.5, −11.6, +0.5, and +4.4 ppm). A MALDI-TOF MS analysis indicated that poly-**3*** was made of oligomers with two to four repeat units (Table 4).

No reaction was observed upon heating **2d** to 235 °C for 28 days. However, 1,4-polymerization did take place upon heating this diacetylene to 300 °C for 24 h. An IR spectroscopic analysis of the final solid showed that the $\nu_{C\equiv C}$ of **2d** (2070 cm^{-1}) had been replaced by a new vibration at 2145 cm^{-1}, assigned to the $\nu_{C\equiv C}$ of an enyne structure. No additional band was observed near 1880 cm^{-1}, suggesting the absence of triene units. The solid-state ^{29}Si NMR spectrum was complex and exhibited four intense resonances at δ = −29.3, −19.5, −12.8, and +0.1 ppm, corresponding to $SiPh_3$ groups in different environments. The solid-state ^{13}C NMR spectrum showed two signals in the aromatic region at 127.8 and 135.2 ppm accompanied by a hump, at the base of the peak at 135.2 ppm, assigned to the sp^2 carbons of an enyne structure ($\delta \approx$ 150 ppm). A MALDI-TOF MS analysis of poly-**2d** did not provide any exploitable information.

Molten-state polymerization of diacetylenes bearing Si−H bonds was also studied. The presence of a hydrogen atom on silicon was expected to have some impact on sterics and perhaps modify the course of the polymerization process (i.e., 1,2- instead of 1,4-addition). Additionally, Si−H bonds are known to add to unsaturated systems, so it is important to assess their reactivity upon heating. Volatile $Me_2HSiC{\equiv}CC{\equiv}CSiHMe_2$ (**5a**)

was heated to 200 °C for 5 h (see Table 3). The IR spectrum of the final solid showed the absence of bands due to the C≡CC≡C fragment of **5a** (2073 and 2050 cm^{-1})[17] and the presence of two new vibrations at 2126 and 1883 cm^{-1}. The 1883 cm^{-1} band arises from triene units. The 2126 cm^{-1} vibration is a superposition of the $\nu_{C\equiv C}$ band of enyne structural motifs and the ν_{Si-H} band of $SiMe_2H$ groups ($\nu_{Si-H} = 2150$ cm^{-1} for **5a**). A solution ^{13}C NMR analysis confirmed the presence of enyne and butatriene structures: two small humps were observed at $\delta \approx 100$ and 110 ppm along with a broad signal, centered at $\delta \approx 140$ ppm, spreading from 120 to 160 ppm. The ^{13}C NMR spectrum also displayed three signals near +1 ppm that correspond to $SiMe_2R$ (R ≠ H) moieties, and one signal at −2.6 ppm, assigned to $SiMe_2H$ groups ($\delta(CH_3) = -3.2$ ppm for **5a**). A proton-coupled ^{29}Si NMR analysis confirmed these findings: besides a broad signal centered at −14 ppm, assigned to $SiMe_2R$ (R ≠ H) moieties, a doublet with $J_{SiH} = 200$ Hz was observed at $\delta = -38$ ppm that corresponds to $SiMe_2H$ groups ($\delta(^{29}Si) = -36$ ppm and $^1J_{SiH} = 206$ Hz for **5a**).[17]

A second sample of **5a** was heated to 400 °C for 5 h. In this case, an IR spectroscopic analysis of the final solid showed the presence of enyne and butatriene structures, with the enyne structure being the predominant form. Interestingly, the $\nu_{C\equiv C}$ band of the enyne units is no longer observed at 2126 cm^{-1} but has undergone a slight shift to 2113 cm^{-1}. The aliphatic region of the CP/TOSS ^{13}C NMR spectrum showed a single resonance at +1 ppm, consistent with the presence of $SiMe_2R$ (R ≠ H) moieties, but no signal was observed near −3 ppm, consistent with the absence of $SiMe_2H$ groups. The CP/MAS ^{29}Si NMR spectrum displayed a broad envelope centered at 0 ppm consisting of at least five resonances (−20, −16, −8, 0, and +5 ppm), but no signal was observed near −38 ppm, confirming the absence of $SiMe_2H$ groups.

Similar observations were made upon heating $Ph_2HSiC{\equiv}CC{\equiv}CSiHPh_2$ (**5b**) to 300 °C for 5 h (Table 3): the IR spectrum of the final solid showed the absence of bands due to the C≡CC≡C fragment of **5b** (2065 and 2047 cm^{-1})[17] and the presence of two new vibrations at 2134 and 1890 cm^{-1}. These vibrations are ascribed to enyne and butatriene structures. A DEPT ^{29}Si NMR analysis of the solid confirmed the absence of **5b**, as no resonance was observed near −40 ppm ($\delta(^{29}Si) = -39.6$ ppm and $^1J_{SiH} = 218$ Hz for **5b**).[17] However, a broad and low-intensity signal was observed at $\delta \approx -23$ ppm, consistent with the presence of residual amounts of $SiPh_2H$ groups. These $SiPh_2H$ groups are σ-bonded to an alkenyl-type fragment, as a similar ^{29}Si chemical shift value, −22.11 ppm, has been reported for $Ph_2HSi(CH{=}CH_2)$.[34]

Diyne **7a** was heated to 170 °C for 10 h (see Table 3). The IR spectrum of the resulting black powder showed the absence of the $\nu_{C\equiv C}$ band of **7a** (2040 cm^{-1})[1c] and the presence of two new vibrations at 2109 and 1865 cm^{-1}. These bands originate from enyne (2109 cm^{-1}) and butatriene (1865 cm^{-1}) structural motifs. Similarly to **2a**, the band due to the triene structure was much more intense than the band corresponding to enyne units.

A black powder partly soluble in THF resulted from the heating of $Ph_3SnC{\equiv}CC{\equiv}CSnPh_3$ (**7b**) to 225 °C for 5 h. An IR spectroscopic analysis of the powder showed the absence of the $\nu_{C\equiv C}$ band of **7b** (2044 cm^{-1}) and the presence of three new vibrations at 2120, 1863, and 1577 cm^{-1}. These bands originate from enyne (2120 and 1577 cm^{-1}) and butatriene (1863 cm^{-1}) structural units. Only aromatic signals with chemical shifts comparable to those of the phenyl carbons of **7b**[7] were observed in the solution ^{13}C NMR spectrum of the powder. The CP/MAS ^{13}C NMR spectrum showed the presence of aromatic signals along with a small hump at $\delta \approx 115$ ppm, ascribed to the sp carbons of an enyne skeleton. Solution and solid-state ^{119}Sn NMR analyses provided some unexpected results. The ^{119}Sn NMR spectrum in $CDCl_3$ solution displayed a single resonance at $\delta = -130.8$ ppm. This shift is different from that of **7b** (−170.1 ppm),[7] but identical to that of Ph_4Sn in the same solvent. A narrow line with a chemical shift indistinguishable from that of Ph_4Sn (−120.1 ppm) was observed in the solid-state high-power proton-decoupled ^{119}Sn NMR spectrum of the powder. In the powder X-ray diffractogram, a set of sharp reflections was apparent whose positions and intensities were nearly identical to those of neat Ph_4Sn. These results suggest that cleavage of the Sn−Ph and C_{sp}−Sn bonds takes place when **7b** is heated to 225 °C, leading to the formation of Ph_4Sn. Such phenomenon was not observed upon heating **2d** to 300 °C. Obviously, the greater stability of the Si−C bond as compared to the Sn−C bond is responsible for this dichotomy (for instance, the bond dissociation energy of the $M-C_6H_5$ bond is equal to 85.6 kcal mol^{-1} in Ph_4Si and 62.4 kcal mol^{-1} in Ph_4Sn).[35]

Another sample of **7b** was heated to 200 °C for 5 h. Infrared results similar to those collected with the sample heated to 225 °C were obtained, except that the band due to the butatriene skeleton (1863 cm^{-1}) was much more intense. No band was observed at 2044 cm^{-1}, consistent with the absence of unreacted **7b**. The CP/MAS ^{13}C NMR spectrum displayed two aromatic signals at 128.8 and 137.6 ppm, but no resonance due to enyne or butatriene structures was detected. The solid-state high-power proton-decoupled ^{119}Sn NMR spectrum was quite different from that of the sample heated to 225 °C in that it showed two broad resonances at $\delta = -120$ and −167 ppm. These signals are assigned to polymeric structures resulting from 1,4-addition of the triple bonds of **7b**: the widths at half-height of the signals ($\Delta\nu_{1/2} \approx$ 4200 Hz) are reminiscent of poorly organized systems such as polymers and the observed chemical shifts lie in the range expected for $SnPh_3$ groups bonded to unsaturated fragments ($\delta(^{119}Sn) = -142.2$ ppm for $Ph_3SnCH{=}C{=}CH_2$). Although there is no evidence for the presence of Ph_4Sn in the sample, the presence of this compound cannot be ruled out for the following reasons: first, the line due to Ph_4Sn would be drowned underneath the large resonance at $\delta = -120$ ppm. Second, a powder X-ray diffraction analysis was carried out that showed the absence of lines corresponding to Ph_4Sn, but, because of the limitations of this technique, this result cannot be used to conclude that Ph_4Sn is not present.

(34) Stefanac, T. M.; Brook, M. A.; Stan, R. *Macromolecules* **1996**, *29*, 4549.

(35) Walsh, R. In *The chemistry of functional groups: the chemistry of organic silicon compounds Part 1*; Patai, S., Rappoport, Z., Eds.; Wiley: Chichester, U.K., 1989; Chapter 5, pp 371−391.

Scheme 6

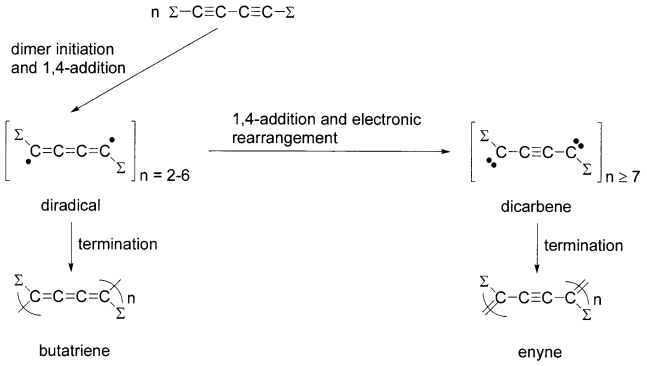

Phosphorus-containing diyne **8** was heated to 180 °C for 2 h (see Table 3). The IR spectrum of the resulting solid showed the absence of the $\nu_{C\equiv C}$ band of **8** (2072 cm^{-1})[18] and the presence of a new vibration at 2111 cm^{-1} due to enyne units. No vibration was observed near 1880 cm^{-1}, consistent with the absence of a triene structure.

The above experimental results call for the following comments: molten-state polymerization of 1,4-bis(triorganosilyl)buta-1,3-diynes leads to polymers with similar structures as those formed during the polymerization of alkyl- and aryl-substituted diynes[8a−h,11,13,24] and poly[(silylene)diethynylenes],[9a,b] suggesting that disilylated diacetylenes also polymerize via a 1,4-addition mechanism. The same is true for $R_2HSiC{\equiv}CC{\equiv}CSiHR_2$ and $R_3SnC{\equiv}CC{\equiv}CSnR_3$ compounds and for $Ph_2PC{\equiv}CC{\equiv}CPPh_2$.

A large number of studies dealing with the identification of intermediates involved in diacetylene polymerization have been published in the literature, the results of which may be summarized as follows (Scheme 6): at the beginning of the polymerization process, propagation proceeds via a diradical mechanism (which gives butatriene structures) up to 6 links; for $n \geq 7$, a dicarbene mechanism is operative that gives enyne structures.[36]

As far as **2a** is concerned, polymers with butatrienic and enyne structures are detected right after the polymerization process has begun, those with a butatrienic skeleton being predominant. As the reaction proceeds, polymers with a butatrienic structure grow more rapidly than those with an enyne structure. A reasonable explanation for these results is that polymers with a butatrienic skeleton and a small number of repeat units form at the very beginning of the experiment. Afterward, these polymers continue to grow as the enyne form, but the chain lengths of these enyne polymers remain small. In other words, during the polymerization reaction, incoming monomer molecules are used mainly to generate short butatriene oligomers rather than enyne polymers with long chains. This conclusion is supported by MALDI-TOF MS results and, also, by the fact that a degree of polymerization of six was found by GPC analysis.[9b]

When the diacetylenic molecule possesses two SiMePhNp moieties (as in **2e** and **2e***) or one SiMePhNp group and one $SiPh_3$ group (as in **3***), the polymers that are detected at the start of the polymerization process have butatrienic and enyne structures, with a predominance of the butatrienic structure. Afterward, the butatriene structure of poly-**2e**/**2e*** develops rapidly and that of poly-**3*** grows slowly. As the end of the reaction gets closer, the populations of the butatrienic forms decrease, whereas those of the enyne forms increase. Considering that the enyne structure gives rise to fairly intense $\nu_{C\equiv C}$ bands in the IR spectra of the final solids, oligomers with numbers of repeat units equal to or greater than seven are expected to be present in significant amounts in poly-**2e**/**2e*** and poly-**3***. This hypothesis is disproved by MALDI-TOF mass spectrometry that shows only oligomers with two to five repeat units. Presumably, the steric bulk of the SiMePhNp and $SiPh_3$ substituents inhibits the formation of oligomers with long chains. Also, to account for the IR results, it is proposed that the presence of these groups favors isomerization of the polymer from the butatrienic structure to the enyne form, in agreement with the fact that the acetylenic backbone is thought to be more stable by ∼12 kcal/mol.[37] Thus, the polymerization results of **2e**/**2e*** and **3*** clearly demonstrate the decisive influence of both steric and electronic factors on diacetylene polymerization in the molten state.

Only the enyne form is detected in the IR spectrum of poly-**2d**. Evidently, the presence of two $SiPh_3$ groups in the starting diacetylene monomer favors exclusively the formation of dicarbene intermediates or, alternatively, makes isomerization of the polymer from the butatrienic structure to the enyne form extremely facile. As a molecular weight distribution could not be obtained by MALDI-TOF mass spectrometry, it is not possible to tell which hypothesis is correct. Nonetheless, these new results fit in nicely with the polymerization results of **2e**/**2e*** and **3*** and reinforce the conclusions drawn from these latter results (vide supra). Nevertheless, the possibility exists that the high reaction temperature (300 °C) may have caused rapid isomerization (<24 h) of the butatrienic skeleton to the enyne structure.

Polymerization of diacetylenes **5a** and **5b** gave polymers that both contained butatriene and enyne structures. In terms of diacetylene polymerization, it may be concluded from this that a $SiHMe_2$ group behaves like a $SiMe_3$ group and a $SiHPh_2$ group also behaves like a $SiMe_3$ group, not like a $SiPh_3$ group.

Diyne **7a** gives polymerization results that are similar to those of **2a**; that is, polymers possessing a butatrienic skeleton are obtained predominantly. Most likely, polymerization of **7a** proceeds via a diradical mechanism as previously suggested in the case of **2a**. This mechanistic similarity is not too surprising given that tin and silicon have identical Pauling electronegativities. Nonetheless, one could have expected the difference in covalent radii between tin and silicon to lead to notably different polymerization results, similarly to what happened concerning the polymerization temperatures (see section 3.1). The polymerization results of **7b** are even more striking, as they are similar to those of **7a** and **2a**. In this case, however, it is not clear whether the fact that the polymerization experiment was run at 200 °C in the solid state was sufficient to modify the final results. Yet, a change in both the electronics and coordination number of the heteroelement borne by the

(36) Sixl, H. *Adv. Polym. Sci.* **1984**, *63*, 49.

(37) Brédas, J. L.; Chance, R. R.; Baughman, R. H.; Silbey, R. *J. Chem. Phys.* **1982**, *76*, 3673.

triple bonds does have dramatic effects on diacetylene polymerization: unlike **7a** and **7b**, molten-state polymerization of **8** gave a polymer with an enyne skeleton, suggesting that polymerization proceeded via dicarbene intermediates (see Scheme 6). Interestingly, dicarbenes derived from **8** would bear some similarity with Bertrand's stable (phosphino)(aryl)carbenes.[38] Thus, for this series of compounds, it can be concluded that the size of the heteroelement, the nature of the substituents bonded to it, and the steric requirements of these substituents have limited impact on the course of diacetylene polymerization as long as the coordination number of the heteroelement is unchanged and its electronegativity remains about the same. These conclusions differ significantly from those drawn previously for the all-silicon series.

3.3. Polymerization Studies of $R_3SiCH_2C{\equiv}CC{\equiv}CCH_2SiR_3$. Insertion of a CH_2 spacer between the triple bonds and the heteroelement is expected to lead to polymerization results that are different from those of 1,3-diynes because the environment of the diacetylene unit is different in terms of both sterics and electronics. Also, polymerization of the latter unit may be altered by propargyl-allenyl-type isomerization. $Me_3SiCH_2C{\equiv}CC{\equiv}CCH_2SiMe_3$ (**4a**) was heated to 235 °C for 4 days (see Table 3), upon which a dark brown powder with a metallic luster was obtained. In the IR spectrum, disappearance of the $\nu_{C\equiv C}$ bands of **4a** was observed (2229 and 2139 cm^{-1}) and a new vibration was detected in the $\nu_{C=C}$ region at 1594 cm^{-1}. The CP/MAS ^{13}C NMR spectrum showed a broad resonance centered at 130 ppm, suggestive of the presence of aromatic carbons in the sample. Methylene groups are detected as a broad signal at 22 ppm and $SiMe_3$ moieties as a fairly sharp resonance at 0 ppm. These results indicate that the formation of polyaromatic-like species with CH_2SiMe_3 dangling groups has occurred. In addition, these species seem to have a regular arrangement, as the CP/MAS ^{29}Si NMR spectrum consists of one fairly sharp resonance at $\delta = 1.8$ ppm. The polymeric mixture consists of oligomers with three to eight repeat units as determined by MALDI-TOF mass spectrometry (Table 4).

The polymerization results of $Ph_3SiCH_2C{\equiv}CC{\equiv}CCH_2SiPh_3$ (**4b**) are more difficult to interpret due to the presence of phenyl substituents on silicon. IR monitoring of the polymerization process did show gradual disappearance of the $\nu_{C\equiv C}$ bands of **4b** (2226 and 2134 cm^{-1}) but, due to the presence of several overtone or combination bands, did not allow unambiguous identification of a new vibration near 1600 cm^{-1}. Interestingly, unlike **4a**, a new band was observed in the $\nu_{C\equiv C}$ region at 2183 cm^{-1}. The CP/MAS ^{13}C NMR spectrum consists of two intense resonances at $\delta = 128$ and 135 ppm due to aromatic carbons and a small hump centered at 15 ppm due to CH_2 groups. The CP/MAS ^{29}Si NMR spectrum exhibits a single resonance at −13.2 ppm along with a small signal at −29.6 ppm, and this simplicity is reminiscent of a fairly organized structure.

Scheme 7

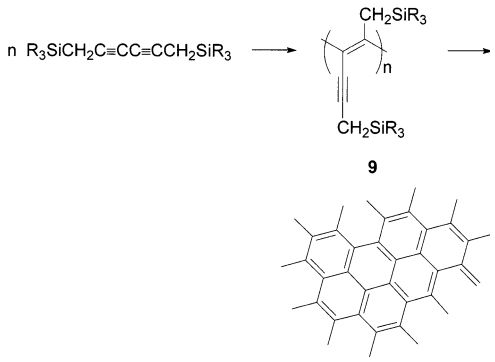

9

Scheme 8

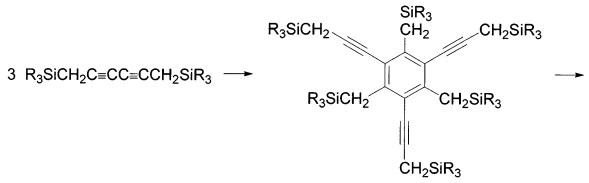

10

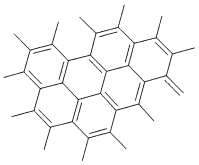

Oligomers with two to four repeat units were observed in the MALDI-TOF mass spectrum of poly-**4b** (Table 4).

Several suggestions can be made as to what the polymerization mechanism of **4a** and **4b** is. It is possible that 1,2-addition polymers form initially that rearrange to polyaromatic structures on further heating (Scheme 7). Such mechanism is inspired from Snow's work[39] on the thermal polymerization of butadiyne and Shim's reports[40] concerning the preparation of condensed cross-linked aromatic structures from acetylenic polyenes bearing CH_2OH substituents.

Alternatively, a cyclotrimerization reaction leading to **10** may be envisioned (Scheme 8).[41] Compound **10** bears some structural similarities with 1,2-addition polymer **9** and, just like it, could lead to a polyaromatic structure on further heating.

Determination of the structure of the final polymer is not a trivial task. As far as **4a** is concerned, solid-state NMR suggests that a well-ordered structure having a large number of CH_2SiMe_3 dangling groups is present, which is in favor of a polyacene such as **11** (Chart 3). Alternatively, structure **12** is possible, but because no vibration is observed in the $\nu_{C\equiv C}$ region of the IR spectrum, this means that further cyclotrimerization must have occurred to completely eliminate the

(38) (a) Despagnet, E.; Gornitzka, H.; Rozhenko, A. B.; Schoeller, W. W.; Bourissou, D.; Bertrand, G. *Angew. Chem., Int. Ed.* **2002**, *41*, 2835. (b) Despagnet, E.; Miqueu, K.; Gornitzka, H.; Dyer, P. W.; Bourissou, D.; Bertrand, G. *J. Am. Chem. Soc.* **2002**, *124*, 11834. (c) Despagnet-Ayoub, E.; Solé, S.; Gornitzka, H.; Rozhenko, A. B.; Schoeller, W. W.; Bourissou, D.; Bertrand, G. *J. Am. Chem. Soc.* **2003**, *125*, 124.

(39) (a) Snow, A. W. *Nature* **1981**, *292*, 40. (b) Snow, A. W. In *Polymer Science and Technology, Vol. 25*: *New Monomers and Polymers*; Culbertson, B. M., Pittman, C. U., Jr., Eds.; Plenum Press: New York, 1984; pp 399−414. (c) Snow, A. W. *J. Macromol. Sci., Chem.* **1985**, *A22*, 1429.

(40) (a) Lee, H. J.; Shim, S. C. *J. Chem. Soc., Chem. Commun.* **1993**, 1420. (b) Lee, H. J.; Shim, S. C. *J. Polym. Sci., Part A*: *Polym. Chem.* **1994**, *32*, 2437. (c) Lee, H. J.; Suh, M. C.; Shim, S. C. *Synth. Met.* **1995**, *71*, 1763. (d) Suh, M. C.; Shim, S. C. *Chem. Mater.* **1997**, *9*, 192.

(41) (a) Vollhardt, K. P. C. *Angew. Chem., Int. Ed. Engl.* **1984**, *23*, 539. (b) Schore, N. E. *Chem. Rev.* **1988**, *88*, 1081. (c) Trost, B. M. *Science* (*Washington, D.C.*) **1991**, *254*, 1471.

Chart 3

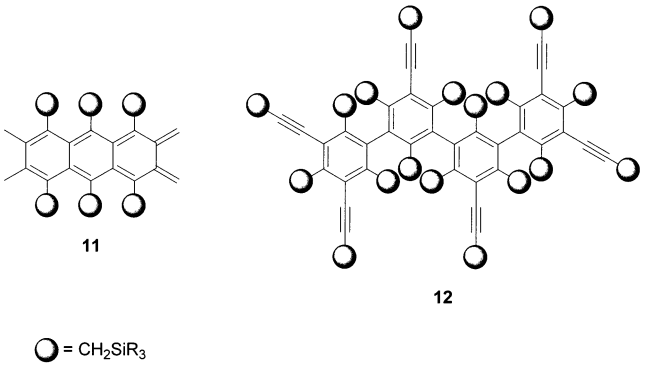

remaining $C{\equiv}CCH_2SiMe_3$ groups. Certainly, the actual structure of the final pyropolymer is quite complex, and as pointed out by Snow in his study of heat-treated polybutadiyne, the transformation of an acetylenic polyene to a polyacene structure appears to be an oversimplification of the real process.[39c]

A vibration is observed at 2183 cm^{-1} in the IR spectrum of poly-**4b**, which suggests that a polyaromatic structure similar to **12** (Chart 3) is obtained. Presumably, the presence of remaining acetylenic linkages in the final polymer is due to the bulkiness of the $SiPh_3$ groups that prevent further cyclotrimerization from occurring.

3.4. Polymerization Studies of $R_3SiC{\equiv}CC{\equiv}CH$. Moving a step further, we wanted to gauge the influence of sterics on diacetylene polymerization in the case where the steric protection of one end of the C_4 rod is minimal. For this reason, molten-state polymerization of **6a**, **6b**, and **6c** was investigated (see Table 3).

$Ph_3SiC{\equiv}CC{\equiv}CH$ (**6b**) was heated to 115 °C for 1 h. The IR spectrum of the resulting solid showed the absence of the $\nu(C_{sp}{-}H)$ and $\nu_{C\equiv C}$ bands of **6b** (3310, 2191, and 2038 cm^{-1}).[22] Concomitantly, a new band was observed at 2154 cm^{-1} that corresponds to the $\nu_{C\equiv C}$ vibration of an enyne skeleton. In the solution ^{29}Si NMR spectrum, an intense resonance is observed at $\delta = -28.7$ ppm. Since this signal has a chemical shift value close to that of **6b** (−28.3 ppm),[22] it is ascribed to $Ph_3SiC{\equiv}C$ moieties. The ^{13}C NMR spectrum in $CDCl_3$ solution exhibits two sets of three signals in the C_{sp} region. The first set (δ = 108.0, 107.3, and 106.7 ppm) is assigned to C_{sp} carbons attached to an unsaturated group; the second set (δ = 96.5, 95.1, and 92.9 ppm) corresponds to C_{sp} carbons bonded to silicon. In the region of the spectrum corresponding to aromatic carbons, four new peaks are observed as compared with that of **6b**.[22]

The above results are consistent with 1,2- rather than 1,4-polymerization of the triple bonds. A 1,2-addition process has been observed previously by Kobayashi et al. during their study of the polymerization of $Et_3SiC{\equiv}CC{\equiv}CH$ with a Ziegler-Natta-type catalyst (Scheme 9).[42]

Unlike **6a** (vide infra), only the triple bond of **6b** bearing a hydrogen is involved in the polymerization reaction. Evidently, the steric bulk of the Ph_3Si group is responsible for this selectivity. The complexity of the

Scheme 9

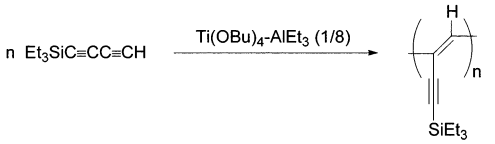

Chart 4

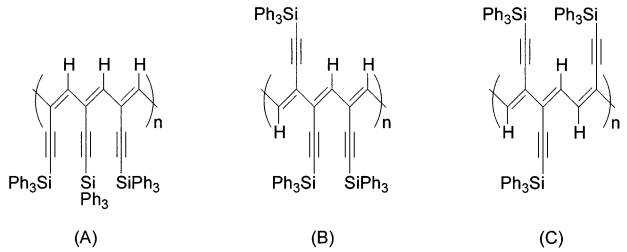

solution ^{13}C NMR spectrum may be rationalized as follows: assuming a trans configuration for each double bond in the backbone, only three triads are possible for poly-**6b** (Chart 4). Triads A and C should each give rise to two signals in the C_{sp} region of the ^{13}C NMR spectrum. Triad B is expected to generate four signals in the same region of the ^{13}C spectrum, but two of them are identical with those of triad C. Thus, a total of six signals is expected to be present in the C_{sp} region of the ^{13}C spectrum, exactly as observed.

A black powder with a metallic luster was recovered upon heating *rac*-$MePhNpSiC{\equiv}CC{\equiv}CH$ (**6c**) to 109 °C for 30 min (see Table 3). In the IR spectrum of the final solid, the $\nu(C_{sp}{-}H)$ and $\nu_{C\equiv C}$ bands of **6c** (3310, 2191, and 2038 cm^{-1}) are no longer observed, and a new band can be seen in the triple bond region at 2154 cm^{-1}. This vibration is ascribed to an enyne structure similar to that of poly-**6b** (vide supra). In the solution ^{13}C NMR spectrum, the C_{sp} carbons of the acetylenic substituents give rise to two sets of three signals. The chemical shifts of these signals are 107.5, 106.8, and 106.2 ppm for the first set and 98.4, 97.0, and 94.8 ppm for the second set. The same region of the CP/MAS ^{13}C NMR spectrum exhibits two broad resonances at δ = 107.8 and 98.0 ppm. The ^{29}Si NMR spectrum in $CDCl_3$ solution consists of three signals with similar intensities and comparable chemical shifts ($\delta = -25.4$, −25.1, and −25.0 ppm). The CP/MAS ^{29}Si NMR spectrum is more complex and shows two strong resonances in a 2:1 ratio at −27.8 and −23.0 ppm accompanied by two smaller and broader signals at −15.7 and −9.2 ppm. Oligomers with three to 10 repeat units were observed in the MALDI-TOF mass spectrum of poly-**6c** (Table 4).

The case of $Me_3SiC{\equiv}CC{\equiv}CH$ (**6a**) is more complex. In a first experiment, diyne **6a** was heated to 50 °C for 6 h. The IR spectrum of the product showed the presence of **6a** (3313, 2189, and 2039 cm^{-1}) and a polymer with an enyne skeleton (2154 cm^{-1}). This polymer is believed to have structure D (Chart 5). Also, a second band is observed near the 3313 cm^{-1} vibration due to **6a** that is assigned to a polymer with an acetylenic hydrogen. This second polymer is believed to have structure E. The solid-state ^{29}Si NMR data agree with the IR results: besides an intense resonance at −17.7 ppm due to species possessing $Me_3SiC{\equiv}C$ moieties (**6a** and enyne polymer D), a broad signal is observed at $\delta \approx -3.5$ ppm that corresponds to enyne polymer E. The CP/TOSS ^{13}C

(42) (a) Kobayashi, N.; Nakada, M.; Tsuchida, E.; Matsuda, H.; Nakanishi, H.; Kato, M. *J. Polym. Sci., Part C: Polym. Lett.* **1986**, *24*, 215. (b) Kobayashi, N.; Nakada, M.; Ohno, H.; Tsuchida, E.; Matsuda, H.; Nakanishi, H.; Kato, M. *New Polym. Mater.* **1987**, *1*, 3.

Chart 5

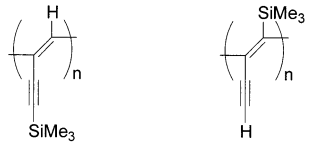

(D) (E)

spectrum displays a single resonance at +0.6 ppm due to Me_3Si groups, but no signal due to sp^2 and sp^3 carbons is detected. Thus, the steric bulk of the Me_3Si group is not sufficient to lead exclusively to the formation of structure D, enabling the formation of structure E.

A second sample of **6a** was heated to 110 °C for 2 h. An IR spectroscopic analysis of the final solid shows that **6a** and enyne structure E are absent (no absorption is detected near 3310 cm^{-1}). The $\nu_{C\equiv C}$ vibration of enyne structure D is observed (2147 cm^{-1}) along with a new band at 1889 cm^{-1} corresponding to a triene skeleton. The origin of the triene structure is unclear: perhaps it originates from unreacted **6a** still present in the sealed tube at 50 °C or from thermal rearrangement of enyne polymer E. The CP/TOSS ^{13}C spectrum of the solid exhibits one intense resonance at 0.3 ppm due to Me_3Si groups, one broad resonance at 103 ppm due to sp carbons, and one broad signal centered at 130 ppm due to sp^2 carbons. The CP/MAS ^{29}Si NMR spectrum is more complex than expected from the IR data: it shows one intense resonance at −18.2 ppm due to $Me_3SiC\equiv C$ moieties, two broad signals at $\delta \approx -7$ ppm and $\delta = -3.4$ ppm, and one broad resonance at $\delta = +2.9$ ppm. The enyne polymer persists when the sample is heated to 400 °C, but the triene structure does not.

Conclusion

The 1,4-bis(triorganosilyl)buta-1,3-diynes studied in this work showed no solid-state polymerization activity. Characterization of several of them by single-crystal X-ray diffraction shows that this is because the $R_{1,4}$ and γ values are not in the correct range. Hence, it appears that the criteria for topochemical polymerization previously established for purely organic diacetylenes also apply to these diynes.[8] $R_3SiC\equiv CC\equiv CSiR_3$ derivatives polymerize thermally in the molten state to give mixtures of small oligomers as determined by MALDI-TOF mass spectrometry. Characterization of these oligomers by infrared and solution and solid-state multinuclear NMR spectroscopies gives evidence that enyne and butatriene structural units are present, a proof that polymerization proceeds via a 1,4-addition mechanism.[8a−h,11,13,24] Similar results were obtained with stannyl- and phosphanyl-terminated diynes. It was also found that when methyl groups are attached to the heteroelement, oligomers with butatrienic structures are generally favored. On the other hand, oligomers with enyne structures are favored with diacetylenes bearing aromatic groups. Furthermore, and consistent with previous literature results, butatrienic structures appear to be predominant at the beginning of the polymerization reaction or when the polymerization experiment is run at low temperature. Molten-state polymerization of $R_3SiCH_2C\equiv CC\equiv CCH_2SiR_3$ compounds does not proceed via diradical or dicarbene intermediates but is thought to proceed via acetylenic polyenes or structures arising from cyclotrimerization of the starting diyne. Ultimately, polyacene or polyaromatic structures with $C\equiv CCH_2SiR_3$ dangling groups are obtained, depending on the nature of R. In the case of $R_3SiC\equiv CC\equiv CH$ derivatives, polymerization occurs via a 1,2-addition process, giving acetylenic polyenes.

Experimental Section

General Considerations. All manipulations were carried out under an inert atmosphere of dinitrogen or argon using standard Schlenk-line techniques. Tetrahydrofuran (THF) and diethyl ether (Et_2O) were distilled over sodium-benzophenone ketyl prior to use.

Solution ^1H, ^{13}C, ^{29}Si, and ^{119}Sn NMR spectra were obtained on Bruker instruments of the following types: AW 80, WP 200 SY, Avance DPX 200, AC 250, and Avance DRX 400. Chemical shifts were referenced as follows: ^1H (protio impurities of the NMR solvents or Me_4Si), ^{13}C (NMR solvents), ^{29}Si (Me_4Si), ^{119}Sn (Me_4Sn). Solid-state ^{13}C, ^{29}Si, and ^{119}Sn magic-angle spinning (MAS) and cross-polarization magic-angle spinning (CP/MAS) NMR spectra were recorded on Bruker ASX 200, AM 300, and ASX 400 spectrometers using 4 or 7 mm zirconia rotors. Spinning rates ranged from 3 to 12 kHz. Carbon and silicon chemical shifts were referenced with an external sample of tetramethylsilane and tin chemical shifts with an external sample of tetramethyltin. Infrared spectra were recorded on a Perkin-Elmer 1600 FT-IR spectrometer with a 4 cm^{-1} resolution. Electron impact (EI) mass spectra were obtained on a JEOL JMS-DX300 instrument. MALDI-TOF mass spectra were obtained on a Bruker ProFlex III spectrometer equipped with a N_2 laser system (337 nm) to desorb and ionize analyte molecules. Polymer samples were dissolved in CH_2Cl_2, and dithranol was used as a matrix. All reported data were acquired using the linear positive-ion mode at +20 kV. Melting points were measured on a Gallenkamp melting point apparatus and are uncorrected. DSC experiments (other than those concerning solid-state polymerization studies) were carried out under nitrogen on a Mettler 30 instrument with a heating rate of 5 °C/min. X-ray powder patterns were obtained using Cu Kα radiation on a Philips diffractometer interfaced with a multiacquisition computerized system developed by Prof. R. Fourcade (Université Montpellier II).[43] Elemental analyses were carried out at the Laboratoire de Microanalyse of the Ecole Nationale Supérieure de Chimie de Montpellier (ENSCM) or at the Service Central de Microanalyse of the Centre National de la Recherche Scientifique (CNRS), Vernaison, France.

Materials. The following chemicals were used as supplied: 2.5 M solution of *n*-BuLi in hexanes (Acros Organics), 2 M solution of LDA in THF−*n*-heptane (Acros Organics), 1.5 M solution of MeLi−LiBr in diethyl ether (Aldrich).

(*Z*)-$CH_3OCH{=}CHC{\equiv}CH$ was purchased from Aldrich, purified as described in the literature,[44] and distilled from CaH_2. $Me_3SiC{\equiv}CC{\equiv}CSiMe_3$ (**2a**),[16] $Me_2PhSiC{\equiv}CC{\equiv}CSiPhMe_2$ (**2b**),[17] $MePh_2SiC{\equiv}CC{\equiv}CSiPh_2Me$ (**2c**),[17] $Ph_3SiC{\equiv}CC{\equiv}CSiPh_3$ (**2d**),[17] $Me_2HSiC{\equiv}CC{\equiv}CSiHMe_2$ (**5a**),[17] $Ph_2HSiC{\equiv}CC{\equiv}CSiHPh_2$ (**5b**),[17] (*R*)-(+)-$Ph_3SiC{\equiv}CC{\equiv}CSiMePhNp$ (**3***),[7] $Me_3SiC{\equiv}CC{\equiv}CH$ (**6a**),[19,20] $Ph_3SiC{\equiv}CC{\equiv}CH$ (**6b**),[22] $Me_3SnC{\equiv}CC{\equiv}CSnMe_3$ (**7a**),[7] $Ph_3SnC{\equiv}CC{\equiv}CSnPh_3$ (**7b**),[17] $Ph_2PC{\equiv}CC{\equiv}CPPh_2$ (**8**),[18] $Me_3SiCH_2C{\equiv}CH$,[45,46] and $Ph_3SiCH_2C{\equiv}CH$[45,47] were prepared by literature methods. *rac*-MePhNpSiCl was synthesized by following the same procedure as that reported for (*S*)-(−)-

(43) Fourcade, R.; Ducourant, B.; Mascherpa, G. CNRS-ANVAR license 5706-00, 1988.

(44) Corey, E. J.; Albright, J. O. *J. Org. Chem.* **1983**, *48*, 2114.

(45) (a) Le Quan, M.; Billiotte, J.-C.; Cadiot, P. *C. R. Acad. Sci.* **1960**, *251*, 730. (b) Masson, J.-C.; Le Quan, M.; Cadiot, P. *Bull. Soc. Chim. Fr.* **1967**, 777.

MePhNpSiCl[7] except that no (1*R*,2*S*)-(−)-ephedrine was used in the synthesis of MePhNpSiH.

Syntheses. *rac*-MePhNpSiC≡CC≡CSiMePhNp (2e). LiC≡CC≡CLi was prepared by the reaction between **2a** and 2 equiv of MeLi−LiBr in THF and allowed to react with *rac*-MePhNpSiCl. After workup, the residual solid was dissolved in a CH_2Cl_2−hexanes mixture (40:60 v/v) and the solution cooled to −18 °C. The precipitate that formed was filtered off and dried in vacuo. Diyne **2e** was obtained as a beige powder in 74% yield. Mp: 149.5−181.5 °C.

^{1}H NMR ($CDCl_3$, 200.1 MHz): δ (ppm) 0.9 (s, 6H, CH_3), 7.4−7.9 (m, 24H, aromatics). ^{13}C NMR ($CDCl_3$, 62.9 MHz): δ (ppm) −0.8 (*C*H_3), 84.3 (C≡*C*Si), 91.9 (*C*≡CSi), 125.6−137.0 (13 signals, aromatics). ^{29}Si NMR ($CDCl_3$, 49.7 MHz): δ (ppm) −24.6. IR (CCl_4): 3071, 3056 ($\nu_{CH\ arom}$), 2965 (ν C_{sp^3}−H), 2069 ($\nu_{C\equiv C}$), 1590, 1430 (phenyls), 1255 (δ_s $SiCH_3$), 1112 (Si−C_{arom}) cm^{-1}. MS (EI, 70 eV): *m*/*z* (assignment, relative intensity) 542 (M^+, 56), 527 ([M − CH_3]$^+$, 55), 295 ([M − SiMePhNp]$^+$, 41), 271 ([MePhNpSiC≡C]$^+$, 67), 247 ([MePhNpSi]$^+$, 95), 168 ([MeNpSi − 2H]$^+$, 100), 154 ([NpSi − H]$^+$, 61), 104 ([PhSi − H]$^+$, 97). Anal. Calcd for $C_{38}H_{30}Si_2$: C, 84.08; H, 5.57; Si, 10.35. Found: C, 84.3; H, 5.7; Si, 10.0.

(*R*,*R*)-(+)-MePhNpSiC≡C≡CSiMePhNp (2e*). Diyne **2e*** was prepared in a fashion similar to **2e** (see above) except that (*S*)-(−)-MePhNpSiCl[7] was used in place of *rac*-MePhNpSiCl. Yield = 72%. Mp: 178.5−180.2 °C. $[\alpha]_D$ = +21.3° (CH_2Cl_2).

On the basis of previous reports by Sommer[48] and Corriu,[49] it was anticipated that the attack of LiC≡CC≡CLi on (*S*)-(−)-MePhNpSiCl would lead to a silane (**2e***) in which the absolute configuration of each silicon center would be *R*. X-ray crystallography has confirmed this (vide infra). An analysis of a bulk sample of **2e*** using a chiral hplc column (the column used was a CHIRALPAK OD, the eluent an hexane−2-propanol mixture (99:1 v/v), and the flow rate 1 mL/min) has also been carried out: the chromatogram showed two peaks at 7.03 and 7.45 min. The first peak corresponds to the meso isomer (9.3%) and the second peak to the (*R*,*R*)-diastereomer (90.7%). The diastereomeric excess is 81.4%.

rac*-Ph_3SiC≡CC≡CSiMePhNp (3).** The same procedure as that leading to (*R*)-(+)-Ph_3SiC≡CC≡CSiMePhNp (**3) was followed[7] except that (*S*)-(−)-MePhNpSiCl was replaced by *rac*-MePhNpSiCl. Yield = 82%. Mp: 148.9−160.4 °C.

Me_3SiCH_2C≡CC≡CCH_2SiMe_3 (4a). Diyne **4a** was prepared by oxidative dimerization of Me_3SiCH_2C≡CH under the Hay conditions.[23] Yield = 68%. Mp: 52.8−54.4 °C.

^{1}H NMR ($CDCl_3$, 250.1 MHz): δ (ppm) 0.1 (s, 18H, CH_3), 1.5 (s, 4H, CH_2). ^{13}C NMR ($CDCl_3$, 62.9 MHz): δ (ppm) −1.6 (*C*H_3), 8.2 (*C*H_2), 64.9 (*C*≡CCH_2), 74.8 (C≡*C*CH_2). ^{29}Si NMR ($CDCl_3$, 49.7 MHz): δ (ppm) 3.5. IR (CCl_4): 2229, 2139 ($\nu_{C\equiv C}$) cm^{-1}. MS (EI, 30 eV): *m*/*z* (assignment, relative intensity) 222 (M^+, 55), 207 ([M − CH_3]$^+$, 60), 149 ([M − $Si(CH_3)_3$]$^+$, 30), 73 ([$Si(CH_3)_3$]$^+$, 100). Anal. Calcd for $C_{12}H_{22}Si_2$: C, 64.79; H, 9.97; Si, 25.25. Found: C, 64.0; H, 9.8; Si, 24.8.

Ph_3SiCH_2C≡CC≡CCH_2SiPh_3 (4b). Diyne **4b** was prepared by oxidative dimerization of Ph_3SiCH_2C≡CH under the Hay conditions.[23] Yield = 86%. Mp: 210.4−216.6 °C.

^{1}H NMR ($CDCl_3$, 200.1 MHz): δ (ppm) 2.4 (s, 4H, CH_2), 7.4−7.6 (m, 30H, aromatics). ^{13}C NMR (solid state, 50.3 MHz): δ (ppm) 5.8 (*C*H_2), 66.7 (*C*≡CCH_2), 73.8 (C≡*C*CH_2), 128.8−137.6 (8 signals, aromatics). ^{29}Si NMR (solid state, 39.7 MHz): δ (ppm) −14.6. IR (KBr): 2226, 2134 ($\nu_{C\equiv C}$) cm^{-1}. MS (EI, 30 eV): *m*/*z* (assignment, relative intensity) 594 (M^+, 9), 516 ([M − C_6H_6]$^+$, 11), 438 ([M − $2C_6H_6$]$^+$, 5), 259 ([$Si(C_6H_5)_3$]$^+$, 100), 105 ([$Si(C_6H_5)$]$^+$, 10). Anal. Calcd for $C_{42}H_{34}Si_2$: C, 84.80; H, 5.76; Si, 9.44. Found: C, 83.9; H, 5.8; Si, 9.6.

***rac*-(*Z*)-CH_3OCH=CHC≡CSiMePhNp.** A procedure similar to that leading to (*Z*)-CH_3OCH=CHC≡$CSi(CH_3)_3$ was followed using *rac*-MePhNpSiCl as the chlorosilane.[16] The title enyne was isolated as an orange oil. Yield = 93%.

^{1}H NMR (CCl_4, 80 MHz): δ (ppm) 0.8 (s, 3H, CH_3), 3.6 (s, 3H, CH_3O), 4.5 (d, $^3J_{HH}$ = 6.4 Hz, 1H, C*H*C≡C), 6.1 (d, $^3J_{HH}$ = 6.4 Hz, 1H, CH_3OC*H*=), 7.1−8.3 (m, 12H, aromatics). ^{13}C NMR ($CDCl_3$, 62.9 MHz): δ (ppm) −0.3 (*C*H_3), 61.1 (*C*H_3O), 85.8 (*C*HC≡C), 94.8 (C≡*C*Si), 104.3 (*C*≡CSi), 125.6−137.2 (13 signals, aromatics), 158.6 (CH_3OCH=). ^{29}Si NMR ($CDCl_3$, 49.7 MHz): δ (ppm) −26.3. IR (CCl_4): 3072, 3055 ($\nu_{CH\ arom}$), 2963, 2935, 2856 (ν C_{sp^3}−H), 2149 ($\nu_{C\equiv C}$), 1632 ($\nu_{C=C\ aliph}$), 1590, 1429 ($\nu_{C=C\ arom}$), 1272 (ν C_{sp^2}−O), 1256 (δ_s $SiCH_3$), 1117 (Si−C_{arom}) cm^{-1}. Anal. Calcd for $C_{22}H_{20}$OSi: C, 80.44; H, 6.14. Found: C, 79.5;
H, 6.3.

***rac*-MePhNpSiC≡CC≡CH (6c).** Diacetylene **6c** was prepared from *rac*-(*Z*)-CH_3OCH=CHC≡CSiMePhNp by following a reported method.[21] This diyne was isolated as a pinkish precipitate upon crystallization from a CH_2Cl_2−hexanes mixture (40:60 v/v). Yield = 99%. Mp: 103.8−104.7 °C.

^{1}H NMR ($CDCl_3$, 250.1 MHz): δ (ppm) 0.9 (s, 3H, CH_3), 2.2 (s, 1H, *H*C≡C), 7.4−8.1 (m, 12H, aromatics). ^{13}C NMR ($CDCl_3$, 62.9 MHz): δ (ppm) −0.9 (*C*H_3), 68.3 (H*C*≡C), 68.8 (HC≡*C*), 81.9 (C≡*C*Si), 91.2 (*C*≡CSi), 125.6−137.0 (14 signals, aromatics). ^{29}Si NMR ($CDCl_3$, 49.7 MHz): δ (ppm) −24.6. IR (CCl_4): 3310 (ν C_{sp}-H), 3072, 3056 ($\nu_{CH\ arom}$), 2965 (ν C_{sp^3}−H), 2191, 2038 ($\nu_{C\equiv C}$), 1590, 1430 ($\nu_{C=C\ arom}$), 1255 (δ_s $SiCH_3$), 1111 (Si−C_{arom}) cm^{-1}. MS (EI, 70 eV): *m*/*z* (assignment, relative intensity) 296 (M^+, 30), 281 ([M − CH_3]$^+$, 100), 231 ([PhNpSi − H]$^+$, 15), 203 ([M − Me − Ph − H]$^+$, 20), 169 ([M − Np]$^+$, 15), 155 ([NpSi]$^+$, 10), 105 ([PhSi]$^+$, 15), 77 ($C_6H_5^+$, 14). Anal. Calcd for $C_{21}H_{16}$Si: C, 85.09; H, 5.44; Si, 9.47. Found: C, 85.0; H, 5.4; Si, 9.5.

Solid-State Polymerization Experiments. Photochemical polymerization experiments were carried out at the Curie Institute in Paris (France) with use of a ^{137}Cs γ-ray source. In each experiment, the bottom of a small test tube was covered with 25−140 mg of diacetylenic compound and the tube was placed right above the γ-ray source in a cylindrical chamber. Preliminary determination of the amount of γ-rays received by the sample as a function of γ-ray source-to-sample distance and exposure time was done using a calibration method based on photooxidation of Mohr's salt.[50] Each sample was irradiated with a 100 krad dose. Heat-induced solid-state polymerization experiments were carried out on a Setaram DSC-111 differential scanning calorimeter connected to a Hewlett-Packard HP 86 calculator. About 50 mg of diacetylene was used in each run and was placed in a sealed aluminum pan. Temperatures were calibrated against the melting point of naphthalene and energies against the heat of fusion of indium.

Molten-State Polymerization Experiments. A set of thick-walled (2 mm) Pyrex tubes were charged with 50−100 mg of diacetylenic monomer and sealed under vacuum. The tubes were heated at the desired temperature in an oven, a furnace, or an oil-bath. The progress of the polymerization reaction was monitored at regular intervals by opening one of the tubes and recording an infrared spectrum of its contents. Heating was continued until complete disappearance of the starting diacetylene was observed.

Crystal Structure of 2a at 120 K. Data were collected on a Stoe imaging plate diffraction system (IPDS) equipped with an Oxford Cryosystems cryostream cooler device. The crystal-to-detector distance was 70 mm. A total of 192 exposures (3

(46) (a) Pornet, J.; Kolani, N'B.; Mesnard, D.; Miginiac, L.; Jaworski, K. *J. Organomet. Chem.* **1982**, *236*, 177. (b) Brandsma, L. *Studies in Organic Chemistry 34*: *Preparative Acetylenic Chemistry*, 2nd ed.; Elsevier: Amsterdam, 1988; p 127. (c) Nativi, C.; Taddei, M.; Mann, A. *Tetrahedron* **1989**, *45*, 1131.

(47) Majetich, G.; Hull, K.; Casares, A. M.; Khetani, V. *J. Org. Chem.* **1991**, *56*, 3958.

(48) Sommer, L. H.; Korte, W. D. *J. Am. Chem. Soc.* **1967**, *89*, 5802.

(49) (a) Corriu, R.; Royo, G. *Bull. Soc. Chim. Fr.* **1972**, 1490. (b) Corriu, R.; Royo, G. *Bull. Soc. Chim. Fr.* **1972**, 1497.

(50) Fricke, H.; Hart, E. J. In *Radiation Dosimetry*, 2nd ed.; Attix, F. H., Roesch, W. C., Eds.; Academic Press: New York, 1966; Vol. II, Chapter 12, pp 167−239.

min per exposure) were taken in φ movement rotation from 0° to 249.6° with φ increments of 1.3°.[51] No decay corrections were made to the data on the basis of intensity checks of 200 control reflections. The cell parameters were refined from 8000 reflections. Owing to the low value of μ, no absorption correction was made.

The structure was solved by direct methods (SHELXS-97).[52] The SHELXL-97 program was used for full-matrix least-squares refinement against F_o^2 using all reflections.[53] Atomic scattering factors were taken from a standard source.[54] All non-hydrogen atoms were refined anisotropically. Hydrogen atoms were introduced in the calculations with the riding model, with isotropic thermal parameters equal to 1.1 times that of the atom of attachment. Final *R* values and relevant crystallographic data are given in Table 1.

Delaunay reduction of the triclinic unit cell given in Table 1 provided the following cell parameters: $a = 15.986$ Å, $b = 15.960$ Å, $c = 21.967$ Å, $\alpha = 91.02°$, $\beta = 107.21°$, $\gamma = 90.60°$. Evidently, the unit cell obtained after transformation looks very similar to that found at 203 K, but the monoclinic symmetry has disappeared. Furthermore, merging the data using this new cell and space groups with monoclinic symmetries (*C*2, *Cm*, *C*2/*c*, ...) led to R_{eq} values greater than 50% in all cases. Thus, a pseudo-monoclinic symmetry is indeed present in the 120 K phase, but successful refinement of the structure in $P\bar{1}$ confirms the triclinic symmetry of this phase.

Interestingly, the original measurement had been carried out at 150 K; however, the structure could not be solved because we were looking at a mixture of the 120 K phase and the 203 K phase.

Crystal Structure of 2a at 203 K. Data were collected on a Stoe imaging plate diffraction system (IPDS) equipped with an Oxford Cryosystems cryostream cooler device. The crystal-to-detector distance was 70 mm. A total of 179 exposures (3.50 min per exposure) were taken with $0° < \varphi < 250.6°$ and crystal oscillations of 1.4° in φ.[51] No decay corrections were made to the data on the basis of intensity checks of 200 control reflections. The cell parameters were refined from 8000 reflections. Owing to the low value of μ, no absorption correction was made.

Structure solution and refinement methods were identical to those employed in the crystal structure of **2a** at 120 K (see above). Final *R* values and relevant crystallographic data are given in Table 1.

Crystal Structure of 2d at 180 K. Data were collected on a Stoe imaging plate diffraction system (IPDS) equipped with an Oxford Cryosystems cryostream cooler device. The crystal-to-detector distance was 80 mm. A total of 194 exposures (3 min per exposure) were taken in φ movement rotation from 0° to 252.2° with φ increments of 1.4°.[51] No decay corrections were made to the data on the basis of intensity checks of 200 control reflections. The cell parameters were refined from 8000 reflections. Owing to the low value of μ, no absorption correction was made.

Structure solution and refinement methods were identical to those employed in the crystal structure of **2a** at 120 K (see above). Final *R* values and relevant crystallographic data are given in Table 1.

Crystal Structure of 2d at 293 K. Data were collected on a Stoe imaging plate diffraction system (IPDS). The crystal-to-detector distance was 80 mm. A total of 200 exposures (3 min per exposure) were taken with $0° < \varphi < 220.0°$ and crystal oscillations of 1.1° in φ.[51] No decay corrections were made to the data on the basis of intensity checks of 200 control reflections. The cell parameters were refined from 8000 reflections. Owing to the low value of μ, no absorption correction was made.

Structure solution and refinement methods were identical to those employed in the crystal structure of **2a** at 120 K (see above). Final *R* values and relevant crystallographic data are given in Table 1.

Crystal Structure of 2e*. Data were collected at 293 K on an Enraf-Nonius CAD4 automated diffractometer with use of the $\omega-\theta$ scan technique. Lattice constants were determined from a least-squares fit to 21 reflections measured in the range $9.24° < 2\theta < 26.56°$. The intensities of three standard reflections were monitored at intervals of 60 min; no significant change in these intensities was observed. No correction was made for absorption.

The systematic absence ($0k0$, $k = 2n + 1$) is in agreement with space groups $P2_1$ and $P2_1/m$. The non-centrosymmetric space group $P2_1$ was assumed in view of the fact that compound **2e*** was optically active; the correctness of this choice was confirmed by successful refinement of the structure. Direct methods in $P2_1$ (SHELXS-86 program[55]) succeeded in locating the silicon atoms and most of the carbon atoms. The remaining carbons were located in a subsequent difference Fourier map. Only the silicon atoms were refined anisotropically; carbon atoms were refined isotropically. The positions of the hydrogen atoms were calculated (SHELXL-93 program[56]) and taken into account in the refinement on F_o^2. The atomic scattering factors for all atoms were taken from the literature.[54] Final *R* values and relevant crystallographic data are given in Table 1.

Two distinct refinements were conducted in identical ways for the (*R*,*R*) and (*S*,*S*) configurations at silicon. The displayed absolute configuration (*R*,*R*) (see Supporting Information) gave the final residual $R_w = 0.0744$ and the (*S*,*S*) configuration led to $R_w = 0.0747$. This leads to an experimental $\mathscr{R}$ index[57] of 1.00403. The $\mathscr{R}$ index calculated from Hamilton's paper[57] at the 0.01 level of probability is 1.00143.

Crystal Structure of 4a. Data were collected at 163 K on an Enraf-Nonius CAD4 automated diffractometer with use of the $\omega-\theta$ scan technique. Lattice constants were determined from a least-squares fit to 21 reflections measured in the range $15.48° < 2\theta < 49.22°$. The intensities of three standard reflections were monitored at intervals of 60 min; no significant change in these intensities was observed. No correction was made for absorption.

The systematic absence (hkl, $h + k = 2n + 1$) is in agreement with space groups *C*2 and *C*2/*m*. Direct methods in *C*2/*m* (SHELXS-86 program[55]) succeeded in locating all of the non-hydrogen atoms. These atoms were refined anisotropically. The positions of the hydrogen atoms were calculated (SHELXL-93 program[56]) and taken into account in the refinement on F_o^2. The atomic scattering factors for all atoms were taken from the literature.[54] Final *R* values and relevant crystallographic data are given in Table 1.

Crystal Structure of 4b. Data were collected at 293 K on an Enraf-Nonius CAD4 automated diffractometer with use of the $\omega-\theta$ scan technique. Lattice constants were determined from a least-squares fit to 23 reflections measured in the range $8.72° < 2\theta < 26.0°$. The intensities of three standard reflections were monitored at intervals of 60 min; no significant change in these intensities was observed. No correction was made for absorption.

(51) *Stoe IPDS Manual*: *Version 2.87*; Stoe & Cie: Darmstadt, Germany, 1997.

(52) Sheldrick, G. M. *SHELXS-97*: Program for Crystal Structure Solution; University of Göttingen: Göttingen, Germany, 1990.

(53) Sheldrick, G. M. *SHELXL-97*: Program for the Refinement of Crystal Structures from Diffraction Data; University of Göttingen: Göttingen, Germany, 1997.

(54) *International Tables for Crystallography*; Kluwer Academic Publishers: Dordrecht, The Netherlands, 1992; Vol. C, Tables 4.2.6.8 and 6.1.1.4.

(55) Sheldrick, G. M. *SHELXS-86*: A Program for Crystal Structure Solution; Institut für Anorganische Chemie der Universität: Göttingen, Germany, 1986.

(56) Sheldrick, G. M. *SHELXL-93*: Program for the Refinement of Crystal Structures from Diffraction Data; University of Göttingen: Göttingen, Germany, 1993.

(57) Hamilton, W. C. *Acta Crystallogr.* **1965**, *18*, 502.

The systematic absences (hkl, $h + k = 2n + 1$; $h0l$, $l = 2n + 1$) are in agreement with space groups *Cc* and *C*2/*c*. Direct methods in *C*2/*c* (SHELXS-86 program[55]) failed to give a correct solution. Direct methods in *Cc* succeeded in locating the silicon atoms and most of the carbon atoms. The coordinates of these atoms were used as initial values in the refinement of the structure in *C*2/*c*. Only the crystallographically unique silicon atom was refined anisotropically; carbon atoms were refined isotropically. The positions of the hydrogen atoms were calculated (SHELXL-93 program[56]) and taken into account in the refinement on F_o^2. The atomic scattering factors for all atoms were taken from the literature.[54] Final *R* values and relevant crystallographic data are given in Table 1.

Acknowledgment. We wish to thank Prof. R. J. P. Corriu for fruitful discussions and the CNRS and Ministry of National Education for financial support. Chiral Technologies Europe (Illkirch, France) is gratefully acknowledged for the HPLC determination of the optical purity of **2e***. We are thankful to Prof. Michel Schott and Mrs. Jeanne Berrehar from the Groupe de Physique des Solides (Universités Paris 7 et Paris 6, France) for carrying out solid-state polymerization experiments on **2a**, **2e***, **4a**, and **6c**. We also wish to thank Dr. Jean-Michel Barbe from LIMSAG (Dijon, France) for the MALDI-TOF MS analyses of the polymers.

Supporting Information Available: For compounds **2a**, **2d**, **2e***, **4a**, and **4b**: crystal data and details of X-ray diffraction experiments and structure solution; tables of positional and thermal parameters for non-hydrogen and hydrogen atoms; full lists of bond lengths and angles; ZORTEP drawings. This material is available free of charge via the Internet at http://pubs.acs.org.

OM020926A